International Journal of Atmospheric and Oceanic Sciences
2022; 6(1): 13-34
http://www.sciencepublishinggroup.com/j/ijaos
doi: 10.11648/j.ijaos.20220601.13
ISSN: 2640-1142 (Print); ISSN: 2640-1150 (Online)

Temperature, Carbon Dioxide and Methane May Be Linked Through Sea Ice Dynamics

Clive Hambler[1, *], Peter Alan Henderson[1, 2]

[1]Department of Zoology, University of Oxford, Oxford, United Kingdom

[2]Pisces Conservation Ltd, Everton, United Kingdom

Email address:

clive.hambler@zoo.ox.ac.uk (C. Hambler)

[*]Corresponding author

To cite this article:

Clive Hambler, Peter Alan Henderson. Temperature, Carbon Dioxide and Methane May Be Linked Through Sea Ice Dynamics. *International Journal of Atmospheric and Oceanic Sciences*. Vol. 6, No. 1, 2022, pp. 13-34. doi: 10.11648/j.ijaos.20220601.13

Received: May 26, 2022 **Accepted**: June 17, 2022; **Published**: June 27, 2022

Abstract: Background: The seasonal cycle of atmospheric carbon dioxide is usually ascribed to the seasonality of Northern Hemisphere vegetation, and the seasonal cycle of methane is usually ascribed to seasonal removal by the hydroxyl radical. Objective: We test an alternative, that the cycles of these greenhouse gases might be linked to sea ice dynamics. Method: Time-series analysis of carbon dioxide, methane, sea ice parameters, vegetation greenness (NDVI), and temperature. We consider a variable that lags another can not be causal of the leading variable. Results: Carbon dioxide is very strongly correlated with sea ice dynamics, with the carbon dioxide rate at Mauna Loa lagging sea ice extent rate by 7 months. Methane is very strongly correlated with sea ice dynamics, with the global (and Mauna Loa) methane rate lagging sea ice extent rate by 5 months. Sea ice melt rate peaks in very tight synchrony with temperature in each Hemisphere. The very high synchrony of the two gases is most parsimoniously explained by a common causality acting in both Hemispheres. Conclusion: Time lags between variables indicate primary drivers of the gas dynamics are due to solar action on the polar regions, not mid-latitudes as is conventionally believed. Our results are consistent with a proposed role of a high-latitude temperature-dependent abiotic variable such as sea ice in the annual cycles of carbon dioxide and methane. If sea ice does not drive the net flux of these gases, it is a highly precise proxy for whatever does. Potential mechanisms should be investigated urgently.

Keywords: Climate Change, Degassing, Fractionation, Isotope, Outgassing, Productivity

1. Introduction

The atmospheric level of carbon dioxide has risen during the instrumental record [1]. Superimposed on the trend are seasonal cycles. At Mauna Loa, Hawaii, carbon dioxide cycles are very regular and levels typically peak in May of each year, whilst methane, which is less regular, peaks around November. The amplitude of these cycles is generally highest in northern high latitudes, with some recording sites being exceptions and methane variation being more complex in the Northern Hemisphere [2-7].

The seasonal cycle of carbon dioxide is typically ascribed to the cycles of terrestrial productivity on the large land masses of the Northern Hemisphere, generating high seasonal amplitude at Arctic sites such as Barrow and Alert and with low amplitude at the South Pole and other Antarctic sites [1, 8-14]. Similarly, the seasonal cycle of methane is typically ascribed to the cycle of wetland and agricultural and livestock production (with large sources on the land masses of the Northern Hemisphere) and to destruction by the OH radical in summer months in each Hemisphere [2, 3].

However, the seasonal cycles of carbon dioxide and methane are both very strongly correlated with the seasonal cycle of sea ice, suggesting sea ice could have a dominant causal role in the cycle or is extremely strongly correlated with whatever does [6, 7, 15]. This unexpected observation requires explanation and invites the hypothesis that high-latitude temperature drives the dynamics of these gases. Temperature drives ice melt and should thus be very highly correlated with the monthly rate of change of these

greenhouse gasses - whether or not sea ice is involved in the cycles. We test this prediction here.

Temperature is conventionally believed to drive the annual cycles of methane and carbon dioxide through changes in vegetation and microbial productivity, including agriculture [1]. The global carbon dioxide net emission rate has a correlation of 0.77 (significant at the 99.99% level) with lower tropospheric temperature anomaly for the tropical land region [16]. Yet despite great efforts, there is substantial uncertainty in the locations and magnitudes of sources and sinks for these gases [5, 17-26] with polar regions and areas of melting sea ice being amongst the most poorly known due to challenging logistics [27-30].

The locations of sources and sinks of carbon dioxide have traditionally been estimated using 'inversions' and 'atmospheric transport' models which rely on climate models to reverse-engineer from observed gas levels where major fluxes occur (*e.g.* [5, 9, 18, 31-33]). Similarly, for methane, inversions and machine learning models have predicted where and when major ocean-atmosphere fluxes occur (such as shallow and Arctic and biologically productive waters) using sparse samples [3, 5, 21]. We suggest an improvement on this method is to look at the similarity and synchrony of observed monthly rates of change of the gases with observations of potential causal variables, locally and globally. A dominant causal variable should be most strongly correlated with the global rate - with least temporal lag between time-series of the gas rate and its local driver and with co-varying annual amplitudes. Of course, any seasonal variables such as livestock activity or wetland productivity or sea ice extent will have correlations with methane and carbon dioxide seasonality, but the spatial pattern of lags between time-series can help identify the more likely causes and locations. For example, a polar causal variable should have a relatively high correlation and low lag with a positive gas flux near the pole.

Terrestrial productivity in the Northern Hemisphere is typically measured by NDVI [9, 10, 12] which is less strongly correlated with carbon dioxide rates than are sea ice rates [6]; to our knowledge no region has been shown to have extremely high temporal synchrony and hence statistical correlation with the global carbon dioxide rate. A previous study [12] does not present correlations of $r > 0.7$, and includes significance values of $p < 0.1$. A "strong" correlation coefficient of 0.74 between the seasonal cycle amplitude of carbon dioxide and Northern Hemisphere land NDVI was detected [4], with the highest local correlations between carbon dioxide levels and NDVI discovered being $r > 0.9$. Oceanic fluxes have been deduced using a grid showing cohesion between temperature anomaly and carbon dioxide levels at Mauna Loa [34].

Given the relatively strong correlations we have found with sea ice [6, 7] we predict very strong synchrony between polar air temperatures and the high latitude fluxes of methane and carbon dioxide (driven mainly by the annual cycle of solar elevation). We hypothesize high-latitude air temperatures drive sea ice dynamics and snow dynamics and thence might influence greenhouse gas dynamics. Such strong relationships are not presented in the review of the carbon cycle that informs international climate policy [1, 35] and could focus greater attention on high latitude sites and fluxes.

Stable isotope ratios in carbon dioxide have been used to attempt to explain the seasonal variation in carbon dioxide and the contribution of human emissions to the trend in carbon dioxide [8, 11, 36]. The monthly $^{13}C/^{12}C$ ratio co-varies closely and inversely with carbon dioxide in many recording stations, typically attributed to plants selectively fixing ^{12}C in photosynthesis in the Northern Hemisphere land masses, leaving uncertainty on the driver of the seasonal cycle in the Southern Hemisphere [11]. The low proportion of ^{13}C in the Northern Hemisphere is usually attributed to a northern dominance of anthropogenic emission of carbon dioxide from fossil fuel sources which contain high ^{12}C [11].

However, carbon isotopic fractionation can occur by other processes, including microbial digestion and kinetic fractionation of methane [37]. Kinetic fractionation during freezing, degassing and carbonate crystal formation causes a lighter isotopic composition in expelled carbon dioxide whilst ^{13}C is preferentially included in precipitated carbonate [38]. We therefore examine the relationship between sea ice melt and freeze rates and the proportion of the heavy isotope in the atmosphere ($\delta^{13}C$ in CO_2).

An imbalance between positive and negative monthly gas flux rates will lead to accumulation or loss of carbon dioxide in the atmosphere. We therefore also examine changes in rates of net carbon dioxide flux between years - which is known to be correlated with temperature [6, 16, 39].

2. Methods

We use the datasets in Table 1.

Table 1. *Data sources.*

Variable	Data source
Atmospheric CO_2 Mauna Loa, Alert and South Pole Monthly flask	NOAA GML Carbon Cycle Cooperative Global Air Sampling Network, 1983-2019, Version: 2020-07-24 https://www.esrl.noaa.gov/gmd/dv/data/ ftp://aftp.cmdl.noaa.gov/data/trace_gases/co2/flask Accessed 1 August 2020 unless indicated otherwise in figure caption Dlugokencky et al [40]
Barrow, Alaska Monthly flask	Point Barrow: https://scrippsco2.ucsd.edu/data/atmospheric_co2/ptb.html Accessed 20 February 2022 Keeling et al [10]

Variable	Data source
Atmospheric CH_4 Mauna Loa, Alert, Cape Grim and South Pole Monthly flask	NOAA GML Carbon Cycle Cooperative Global Air Sampling Network, 1983-2019, Version: 2020-07-24 https://www.esrl.noaa.gov/gmd/dv/data/ ftp://aftp.cmdl.noaa.gov/data/trace_gases/ch4/flask Accessed 1 August 2020 Dlugokencky et al [41]
Atmospheric CH_4 Globally-averaged monthly data	https://esrl.noaa.gov/gmd/ccgg/trends_ch4/ Accessed 1 January 2021 unless indicated otherwise in figure caption Dlugokencky [42]
Atmospheric stable isotope C13 in CO_2 $\delta^{13}C$ = [(13C/12Csample/($^{13}C/^{12}C$standard/)-1] x 1000 Monthly flask	https://www.esrl.noaa.gov/gmd/dv/data/ Accessed 27 December 2021 White et al [43]
Atmospheric methyl chloroform Gas chromatograph hourly samples	Methyl chloroform data from the NOAA/ESRL halocarbons in situ program https://www.esrl.noaa.gov/gmd/dv/data/ Accessed 29 March 2021
NDVI	MODIS satellite imagery MOD13C2 product as 5 kilometre monthly mean global imagery Accessed July 2019
Sea ice extent Monthly mean	https://nsidc.org/data/seaice_index/archives Sea Ice Index Version 3 ftp://sidads.colorado.edu/DATASETS/NOAA/G02135/ (Fetterer et al [44]) 'North' (= 'Arctic'): ftp://sidads.colorado.edu//DATASETS/NOAA/G02135/north/monthly/data/ at sidads.colorado.edu 'South' (= 'Antarctic'): ftp://sidads.colorado.edu/DATASETS/NOAA/G02135/south/monthly/data/ Files in form: S_01_extent_v3.0.csv Accessed 26 February 2020

Table 1. *Continued.*

Variable	Data source
Sea ice extent Monthly mean	ftp://sidads.colorado.edu/DATASETS/NOAA/G02186/ MASIE NSIDC/NIC Sea Ice Product G02186 - Daily Ice Extent by Region in Square Kilometers National Ice Center and National Snow and Ice Data Center. Compiled by F. Fetterer, M. Savoie, S. Helfrich, and P. Clemente-Colón. 2010, updated daily. Multisensor Analyzed Sea Ice Extent - Northern Hemisphere (MASIE-NH), Version 1. Subset: 4km. Boulder, Colorado USA. NSIDC: National Snow and Ice Data Center. doi: https://doi.org/10.7265/N5GT5K3K Accessed 5 February 2020 unless indicated otherwise in figure caption
Sea ice volume, Arctic Modelled by DMI Monthly mean	http://ocean.dmi.dk/arctic/index.uk.php http://ocean.dmi.dk/arctic/icethickness/txt/IceVol.txt Accessed 23 July 2019
Snow extent Northern Hemisphere Monthly mean	https://climate.rutgers.edu/snowcover/docs.php?target=datareq NH SCE CDR v01r01 https://climate.rutgers.edu/snowcover/files/moncov.namgnld.txt https://climate.rutgers.edu/snowcover/files/moncov.nam.txt Accessed 27 March 2020
Alert air temperature Monthly mean	NCEP Reanalysis Dataset Produced at NOAA Physical Sciences laboratory https://psl.noaa.gov/data/timeseries/arctic/ Accessed 6 January 2021
South Pole air temperature (Amundsen-Scott South Pole Station) Monthly mean	Amundsen_Scott temperature https://legacy.bas.ac.uk/met/READER/surface/Amundsen_Scott.All.temperature.txt British Antarctic Survey. UK Antarctic Surface Meteorology; 1947 - 2013 http://dx.doi.org/10.5285/569d53fb-9b90-47a6-b3ca-26306e696706 Accessed 16 December 2020 unless indicated otherwise in figure caption
Lower Troposphere atmospheric temperature anomaly, Tropical ocean	UAH Temperature Dataset Version 6. Tropics ocean https://www.nsstc.uah.edu/data/msu/v6.0/tlt/uahncdc_lt_6.0.txt Accessed 27 February 2022 Spencer et al [45]

We examine atmospheric gas levels for a site considered globally representative for carbon dioxide (Mauna Loa, Hawaii, USA) [1] and a global average estimate of monthly methane [42]. We also examine methane rates at Mauna Loa since these are measurements from what might also be a representative site for methane.

Within the NOAA Global Monitoring Laboratory network of atmospheric gas recording sites we examine the most northerly site (Alert, Canada) and the most southerly (South Pole) since these would be predicted to respond strongly to any temperature-dependent forcing. Having examined all sites in this network with monthly flask data we selected Cape Grim (Tasmania, Australia, latitude 41°S) as an illustration of the high similarity of phenology of the South Pole to some sites at lower latitudes.

Carbon dioxide records are subject to occasional revision

due to recalibration and other issues [6, 40]. For most sites data are not available for very recent months. We therefore include data from the most northerly site that has recent published data, Point Barrow, Alaska, as provided by the Scripps CO_2 Program (Scripps Institution of Oceanography); these data show more fine detail, and gaps, than monthly data from NOAA which have been more fully processed [6].

We do not use models of atmospheric transport of gas but instead make the minimalistic assumption that gas from a polar region will take longer to reach or cross the equator than to reach nearby sites. We assume the shape of the seasonal gas flux curve will be most similar to the curve of the causal variable near the site of the causal variable (due to mixing).

Temperature data (average monthly values in degrees Centigrade) were obtained for meteorological stations at the South Pole and Alert as examples of very high-latitude sites where local gas levels are also monitored. The Alert data were rescaled by subtracting 100, to make all values negative. Temperature values were inverted to visually compare synchrony of peak temperature with peak negative net fluxes of the gases, since we have previously established peak negative flux is tightly synchronous with sea ice melt at high latitudes [6, 7]. Lower Tropospheric temperature data [45] produced with consistent methods and minimal adjustment since 1978 are compared with annual rate changes for carbon dioxide, updating the time-series in our previous work [6].

Recording of the OH radical in the atmosphere is very difficult, so is usually done indirectly using methyl chloroform (CH_3CCl_3) which OH reacts with and hence lowers the atmospheric concentration [31, 46, 47]. In the annual cycle, low levels of methyl chloroform should correspond to high levels of OH.

We follow the classic use of NDVI to locate likely carbon dioxide fluxes due to terrestrial vegetation productivity [4, 9, 12, 35]. There is high synchrony in monthly NDVI rates between the Northern Hemisphere latitudinal belts and continents [6] and thus for simplicity of presentation we selected data for North America and Eurasia, 35°N to 70°N, which has high amplitude and which captures a substantial area of these continents. Use of NDVI for the full Northern Hemisphere or a narrower high latitude belt would not affect our conclusions [6]. We invert monthly data for NDVI to give an approximate measure of a lack of productivity (indicating periods which have a net carbon dioxide sink). These are rescaled by a factor of 1000 for clarity.

Methodological consistency is essential in time-series analysis [48] so we use datasets which are very likely to have been quality controlled for methodological drift. A monthly database of sea ice extent in named Arctic regions such as the Northern Hemisphere and Greenland Sea is easily available (from NSIDC / MASIE) from January 2006, which we therefore use as the start date for all sea ice time-series. Arctic and Antarctic extents (from NSIDC Sea Ice Index) were used to calculate the rate for the 'global' sea ice extent (which we term 'Arctic plus Antarctic' rate as in previous work [6, 7]). Greenland Sea ice is selected for some comparisons because our initial analysis found it particularly similar in phenology to carbon dioxide in northern high latitudes [6]. Longer time-series are available and presented for selected variables, such as the full continuous carbon dioxide record at Mauna Loa from July 1976, to visually assess if more recent years have a very different pattern. However, long series often have data gaps in different months, which would complicate analysis and preclude direct comparison of correlation strengths; short, consistent time-series are thus used here and are sufficient to reveal very strong correlations.

Rates of change for variables were derived as follows: rate in month 2 is the mean value in month 2 minus the mean value in month 1. The annual average of 12 monthly rates in a year was used to calculate the annual change in average rate in a year: rate in year 2 is the mean value in year 2 minus the mean value in year 1.

Statistical analysis was based on the R platform. Cross correlations and consideration of autocorrelation were performed as in [7]. For pairs of time-series, cross correlations and 95% confidence bounds for lags of up to +/- 12 months were calculated using the ccf function in the tseries R package. These results were used to identify the lag producing the highest correlation and the rcorr function then used to calculate the Pearson correlation and associated probability that it could be generated by random chance. Because we find probabilities are near zero for numerous of our results, which would require many digits to present, significance values are all presented as $p < 0.001$.

Due to data availability and other constraints at the time of this work, some time-series have different end dates or missing values so are not fully comparable and not all are analysed statistically. Statistical analyses are only performed here for the global levels of methane and carbon dioxide and for one other time-series for illustrative purposes (showing a tight visual fit is also supported statistically). The results of any analysis are given in the Figure captions. Our previous work ([6, 7] and unpublished) has established that close visual fits using the minima in such time-series always have high statistical correlations and often identify the lag between them; this can be confirmed if the work is replicated.

3. Results

a) Globally representative atmospheric gas measurements

The monthly time-series for carbon dioxide rate from Mauna Loa, global sea ice extent rate and an Arctic temperature (Alert, Canada) are given in Figures 1-5.

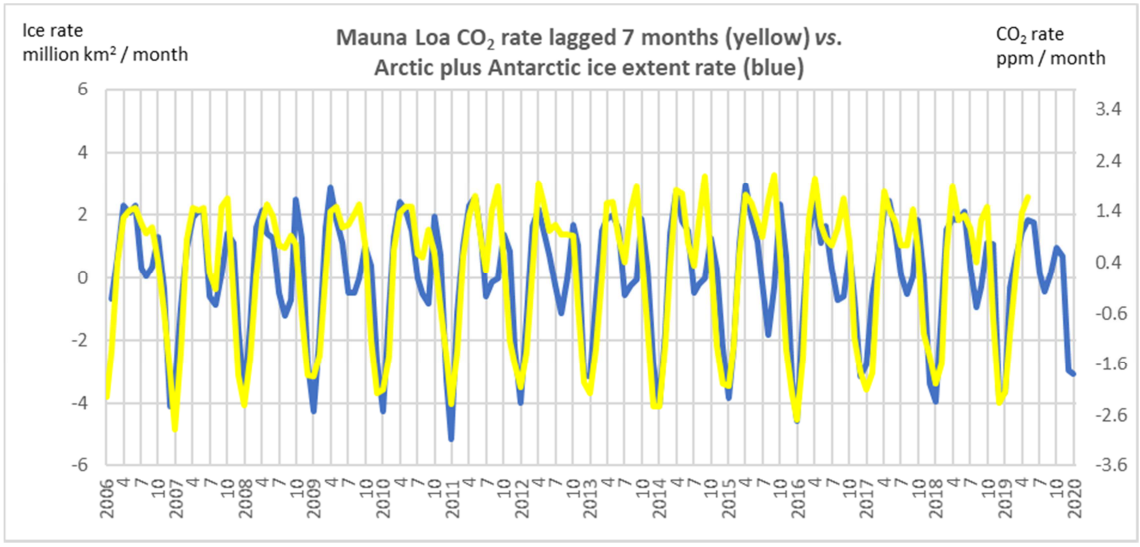

Figure 1. *Global monthly carbon dioxide rate (measured at Mauna Loa, lagged 7 months) vs. global sea ice extent rate. r = 0.79 at lag = 7 months; p < 0.001.*

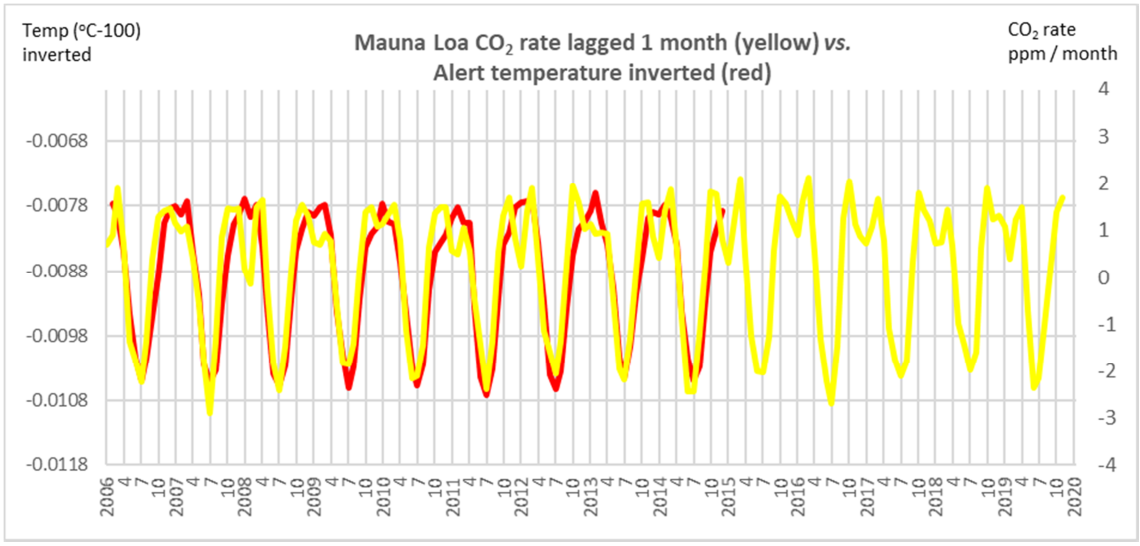

Figure 2. *Monthly carbon dioxide rate Mauna Loa (lagged 1 month) vs. temperature at Alert (inverted).*

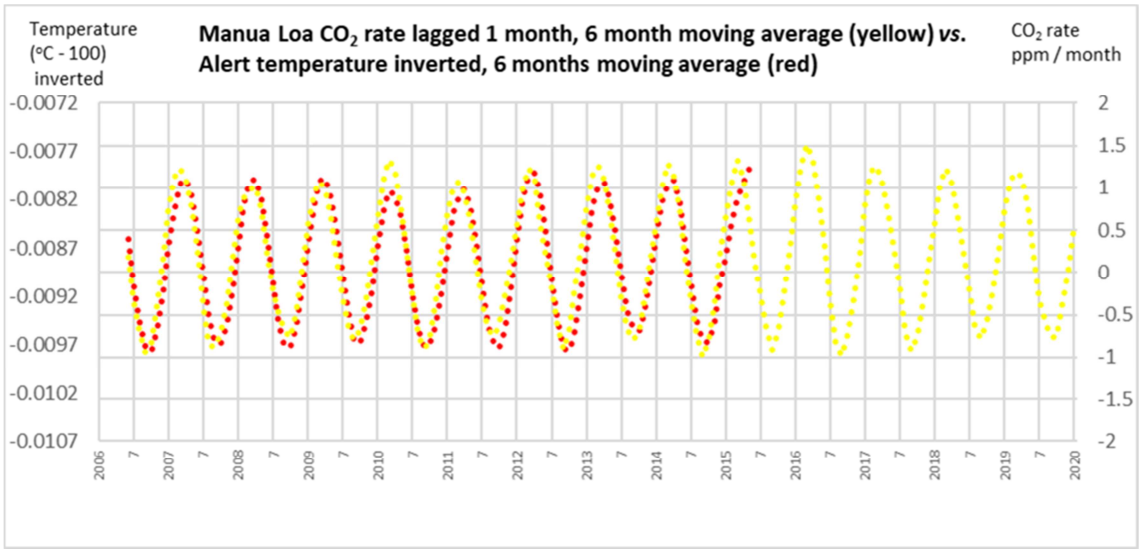

Figure 3. *Monthly carbon dioxide rate Mauna Loa (lagged 1 months) vs. temperature at Alert, Canada (inverted), 6 month moving average for both variables.*

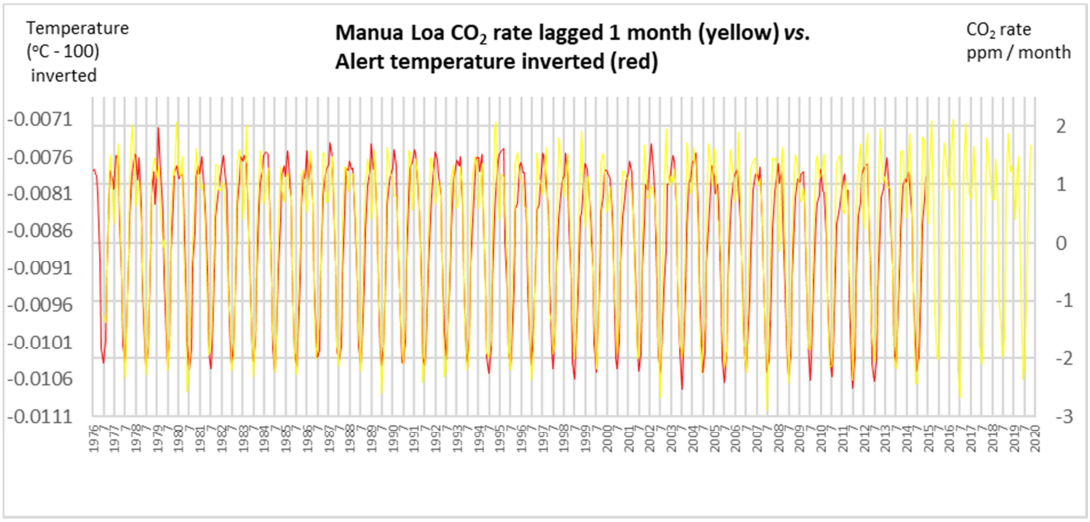

Figure 4. *Monthly carbon dioxide rate Mauna Loa (lagged 1 month) vs. temperature at Alert, Canada (inverted), using full continuous monthly Mauna Loa CO_2 record from July 1976.*

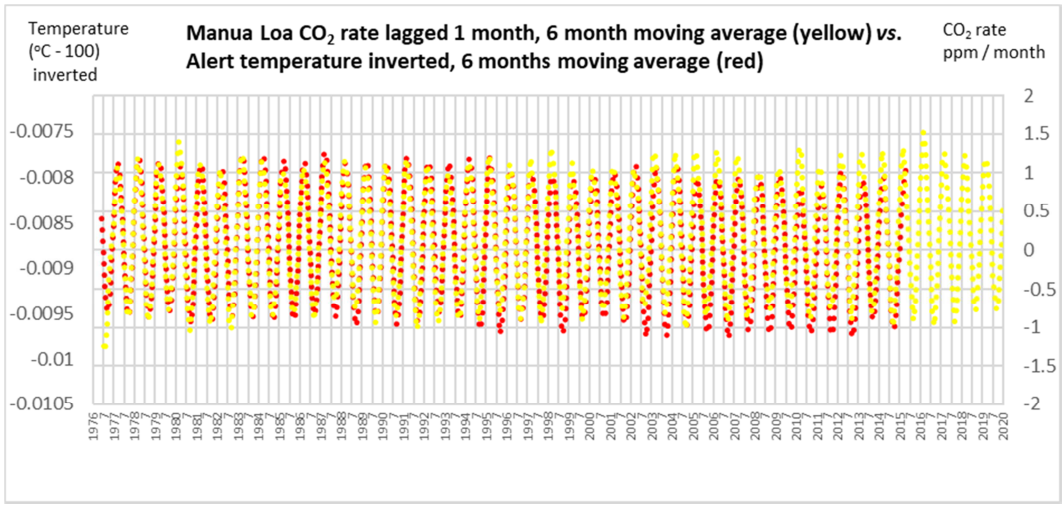

Figure 5. *Monthly carbon dioxide rate Mauna Loa (lagged 1 month) vs. temperature at Alert, Canada (inverted), 6 month moving average for both variables, using full continuous monthly Mauna Loa CO_2 record from July 1976.*

The monthly time-series for carbon dioxide rate from Mauna Loa and an Antarctic temperature (South Pole) are given in Figures 6-8.

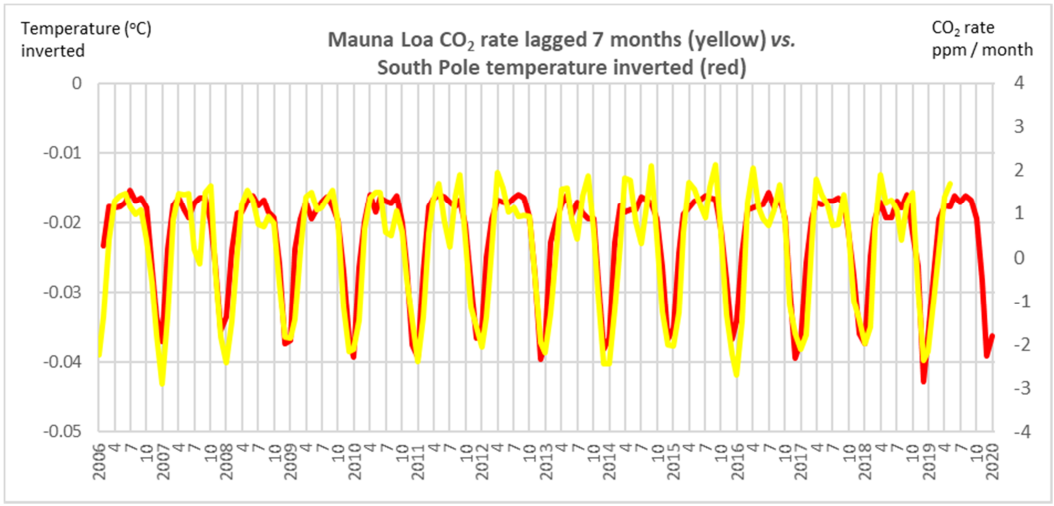

Figure 6. *Monthly carbon dioxide rate Mauna Loa (lagged 7 months) vs. temperature at South Pole (inverted).*

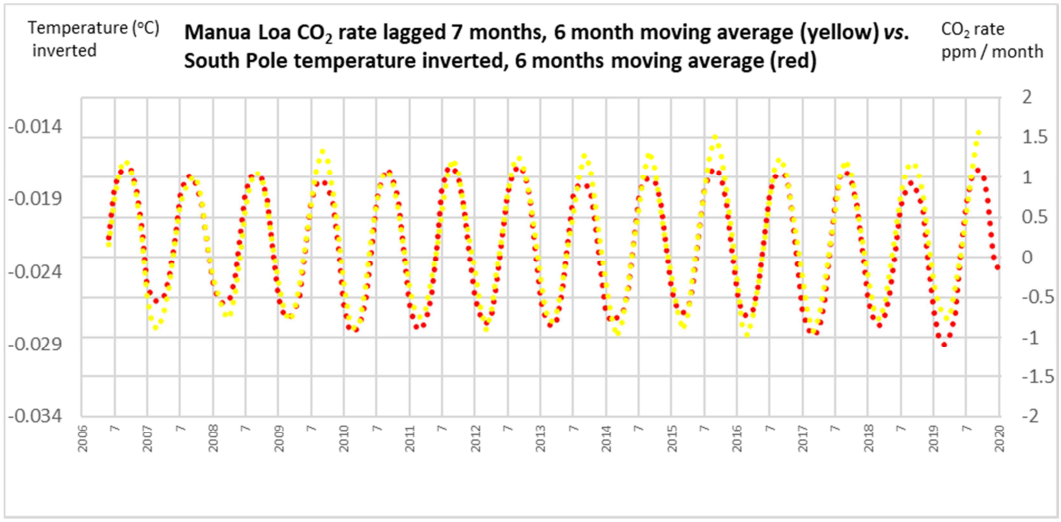

Figure 7. *Monthly carbon dioxide rate Mauna Loa (lagged 7 months) vs. temperature at South Pole (inverted), 6 month moving average for both variables.*

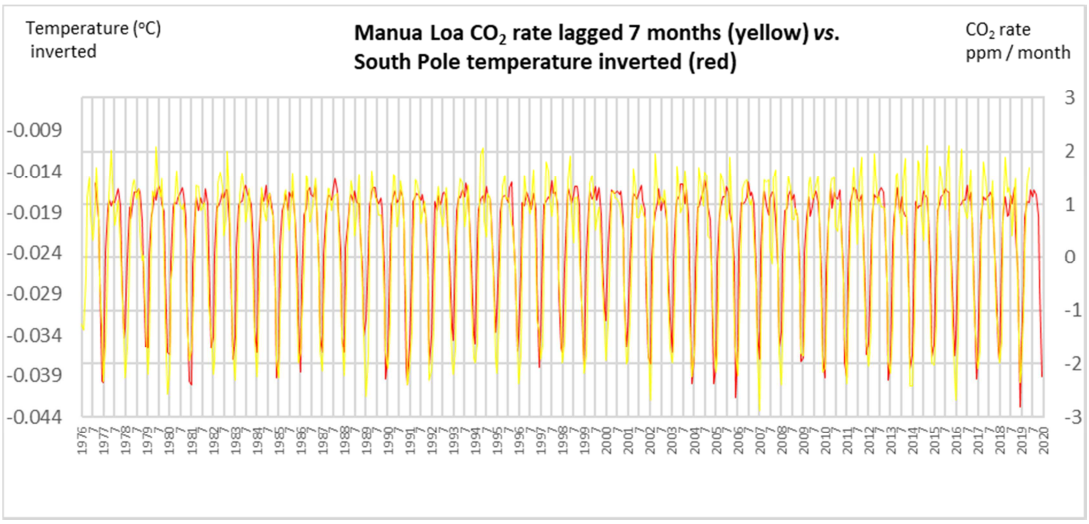

Figure 8. *Monthly carbon dioxide rate Mauna Loa (lagged 7 months) vs. temperature at South Pole (inverted), using full continuous monthly Mauna Loa CO_2 record from July 1976.*

The monthly time-series for methane rates averaged from a global network of sites, and from Mauna Loa, are plotted against global sea ice extent rate in Figures 9-10.

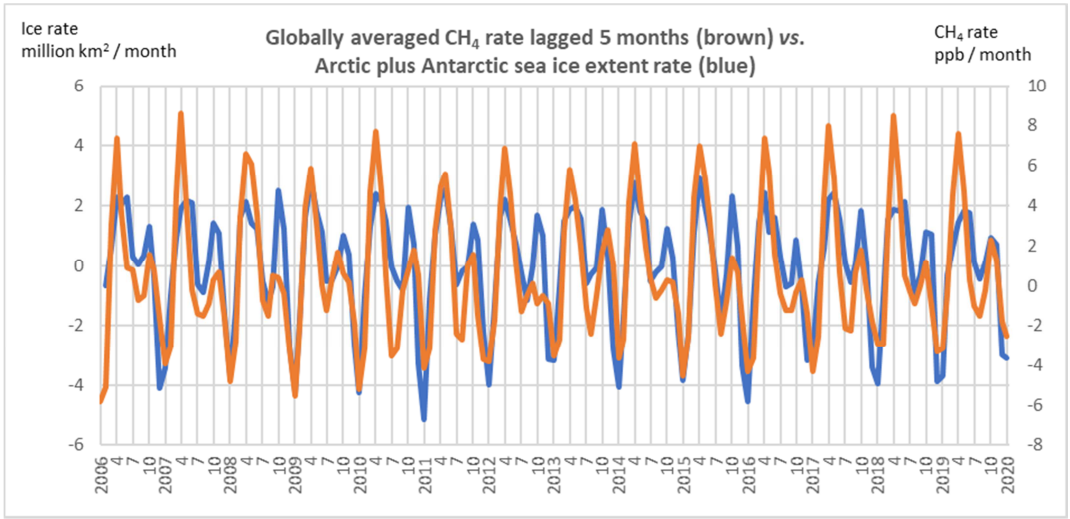

Figure 9. *Monthly global average methane rate (lagged 5 months) vs. global sea ice extent rate. $r = 0.78$ at lag = 5 months; $p < 0.001$.*

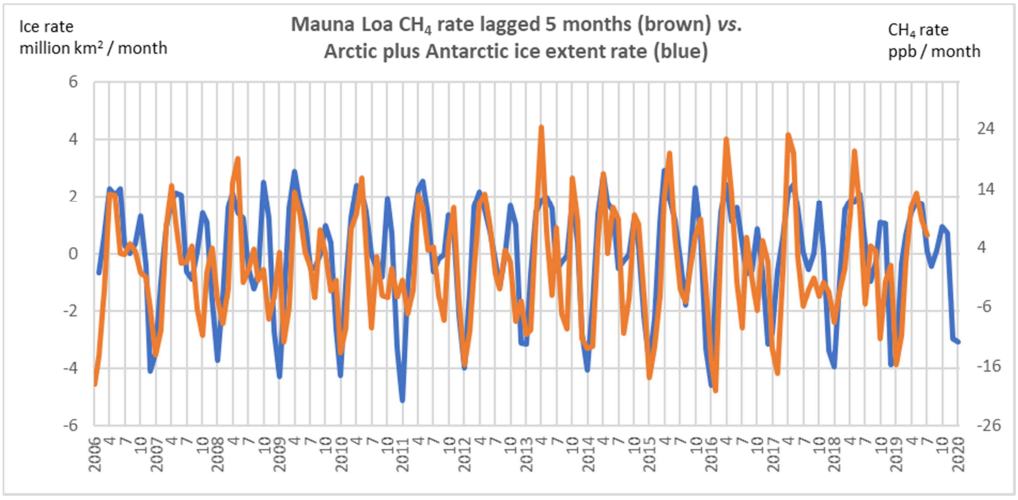

Figure 10. *Monthly methane rate Mauna Loa (lagged 5 months) vs. global sea ice extent rate.*

Globally representative carbon dioxide and methane rates are compared in Figure 11.

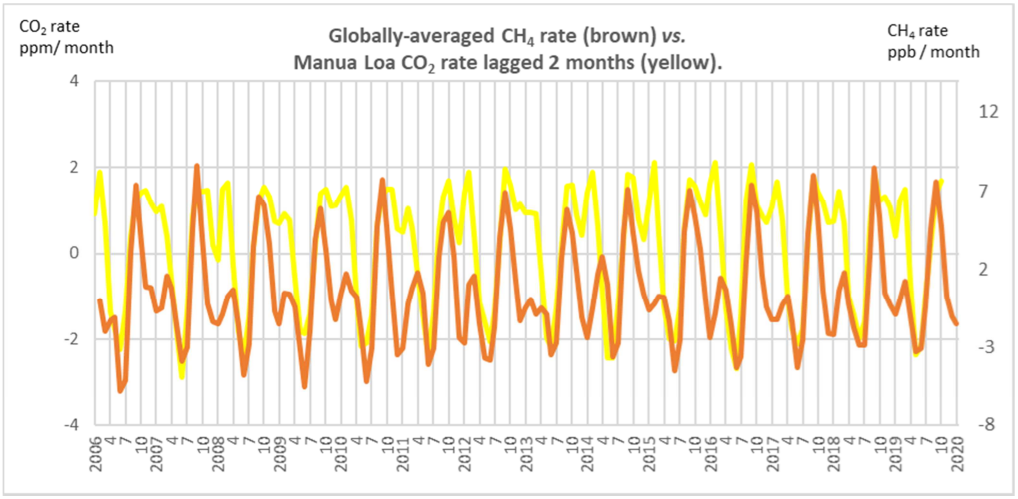

Figure 11. *Global carbon dioxide rate (Mauna Loa, lagged 2 months) vs. global methane rate.*

b) Arctic

Monthly time-series for carbon dioxide and methane rates at Northern Hemisphere high latitude sites are plotted against Alert temperature, Greenland Sea ice extent rate and Northern Hemisphere snow extent rate, in Figures 12-15.

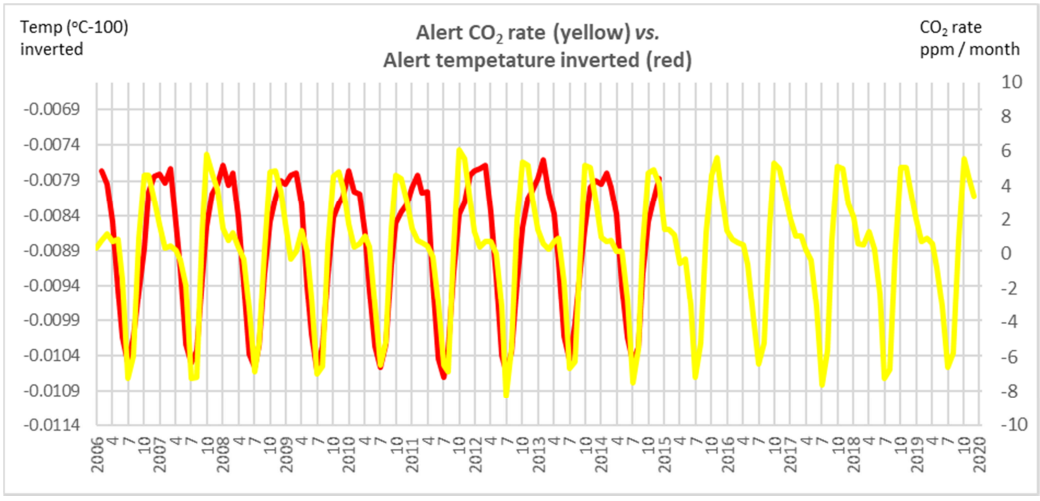

Figure 12. *Monthly carbon dioxide rate Alert, Canada vs. temperature at Alert (inverted).*

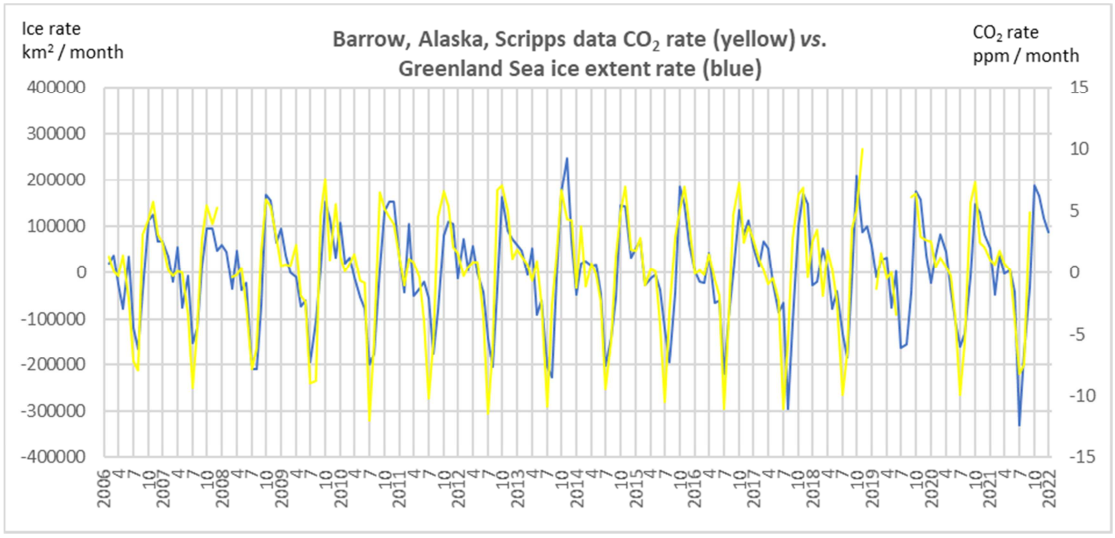

Figure 13. *Monthly carbon dioxide rate at Point Barrow, Alaska (Scripps data) vs. Greenland Sea ice extent rate.*

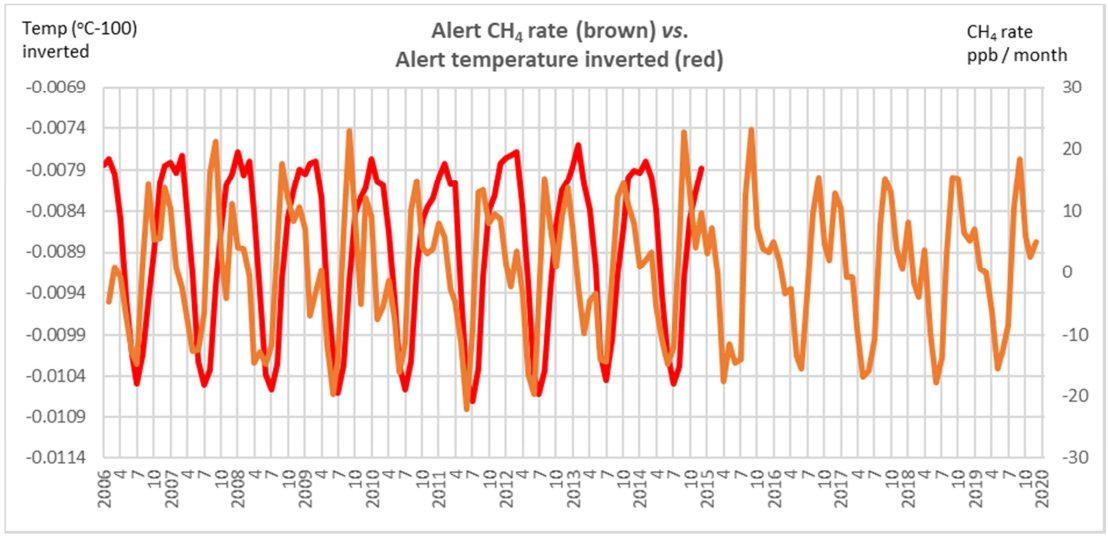

Figure 14. *Monthly methane rate Alert vs. temperature at Alert (inverted).*

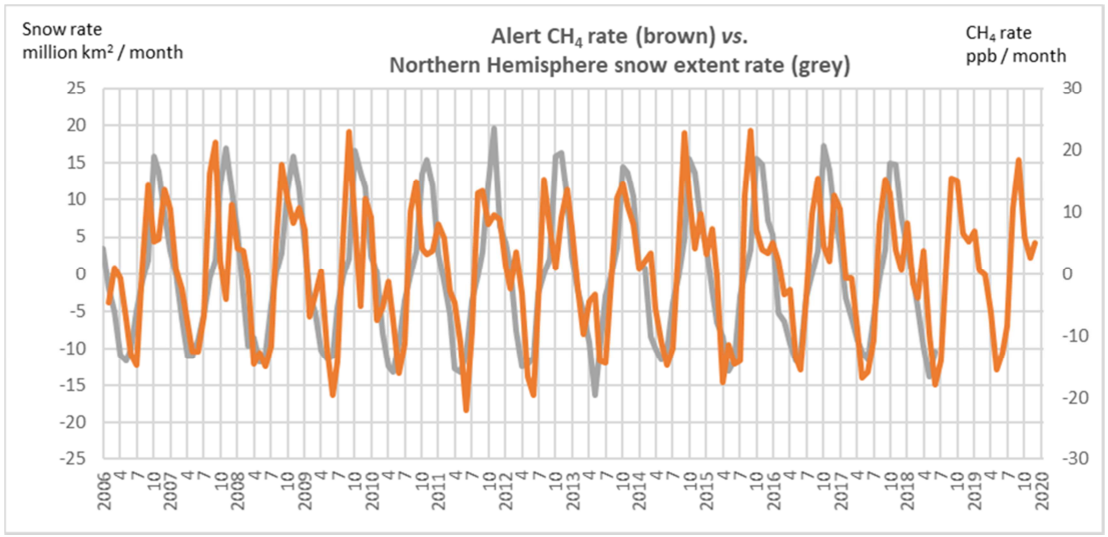

Figure 15. *Monthly methane rate Alert vs. Northern Hemisphere snow extent rate.*

Time-series for Arctic sea ice extent rate and a local temperature (Alert) are given in Figure 16.

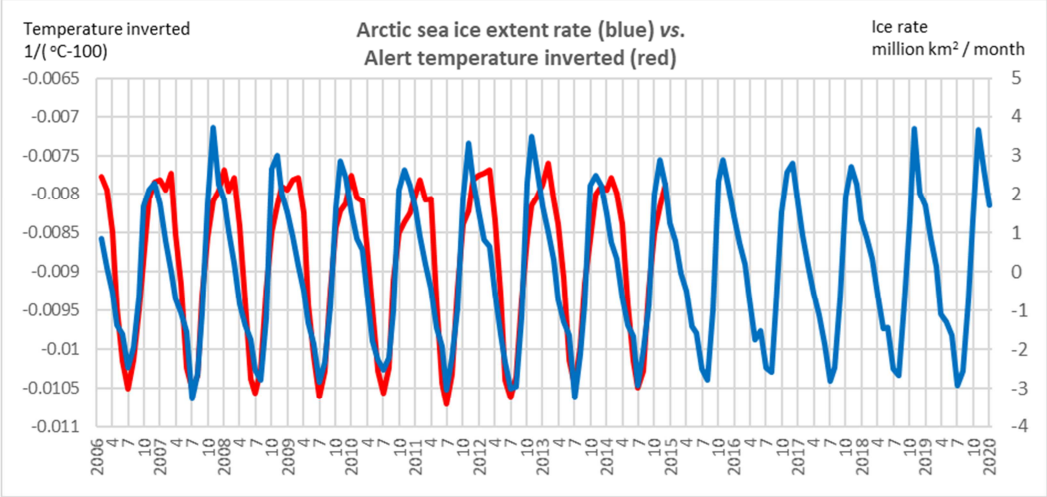

Figure 16. *Monthly Arctic sea ice extent rate vs. temperature at Alert (inverted).*

c) Antarctic

Monthly time-series of carbon dioxide rate and methane rate at the South Pole, and temperature at the South Pole, are given in Figures 17-20.

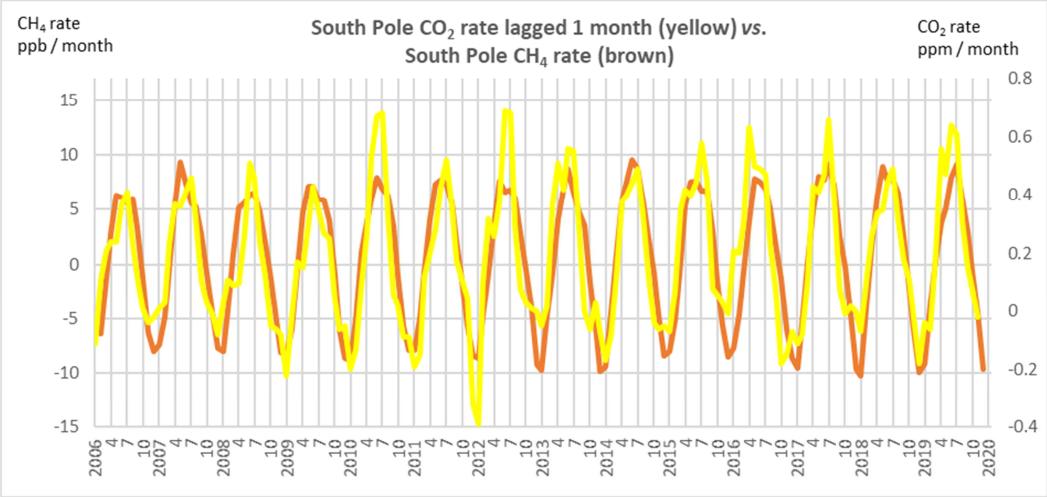

Figure 17. *Monthly carbon dioxide rate South Pole (lagged 1 month) vs. monthly methane rate South Pole.*

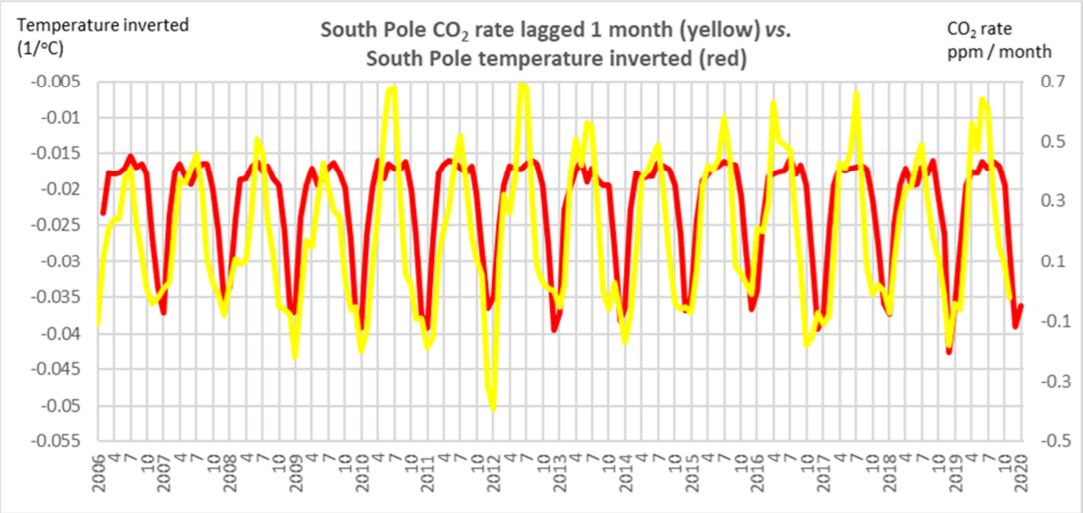

Figure 18. *Monthly carbon dioxide rate South Pole (lagged 1 month) vs. temperature at South Pole (inverted).*

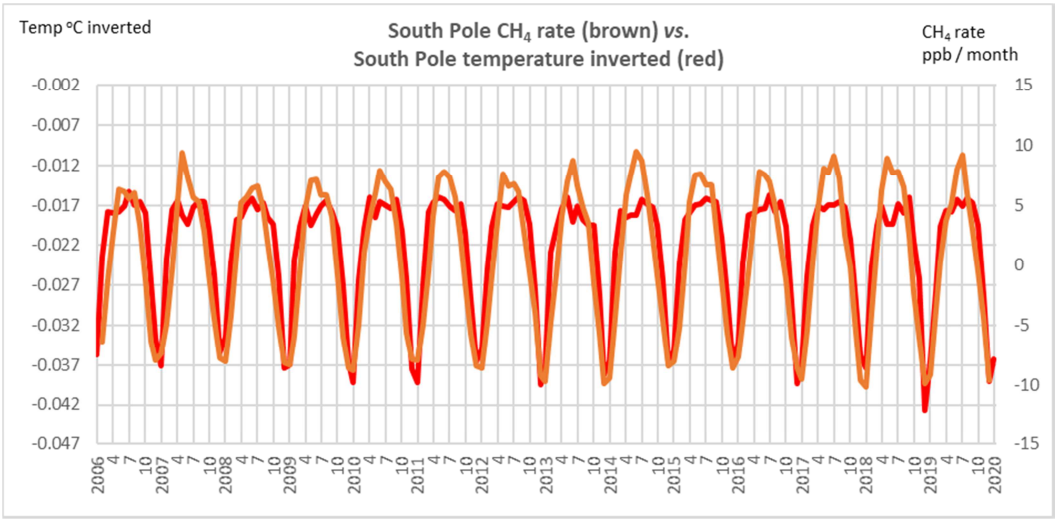

Figure 19. *Monthly methane rate South Pole vs. temperature at South Pole (inverted). r = 0.88 at zero lag; p < 0.001.*

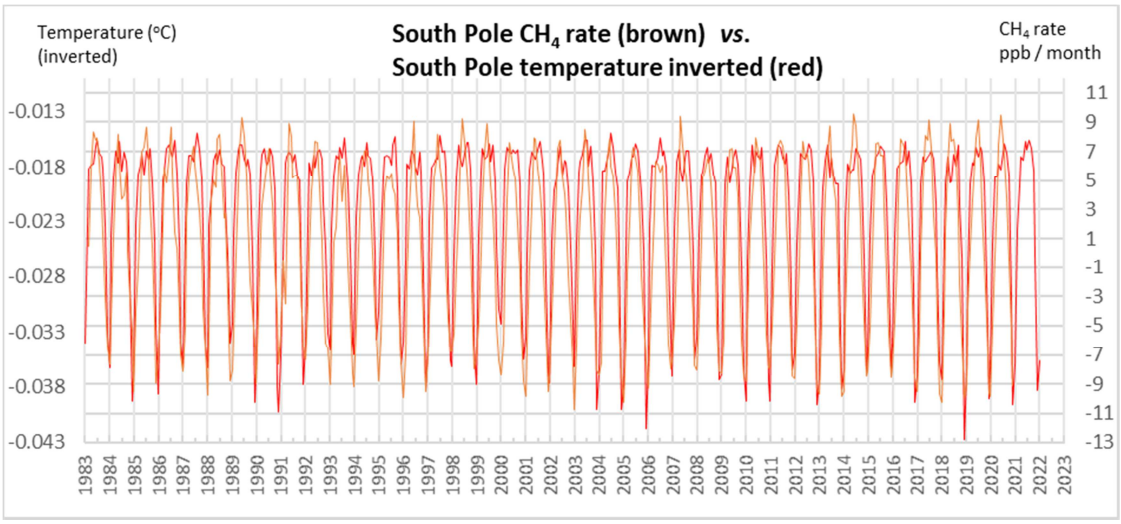

Figure 20. *Monthly South Pole methane rate vs. temperature at South Pole (inverted), using full continuous monthly methane record from February 1983. (Data accessed February 2022).*

An example of the similarity of South Pole methane rate phenology to another Southern Hemisphere site, Cape Grim, is given in Figure 21.

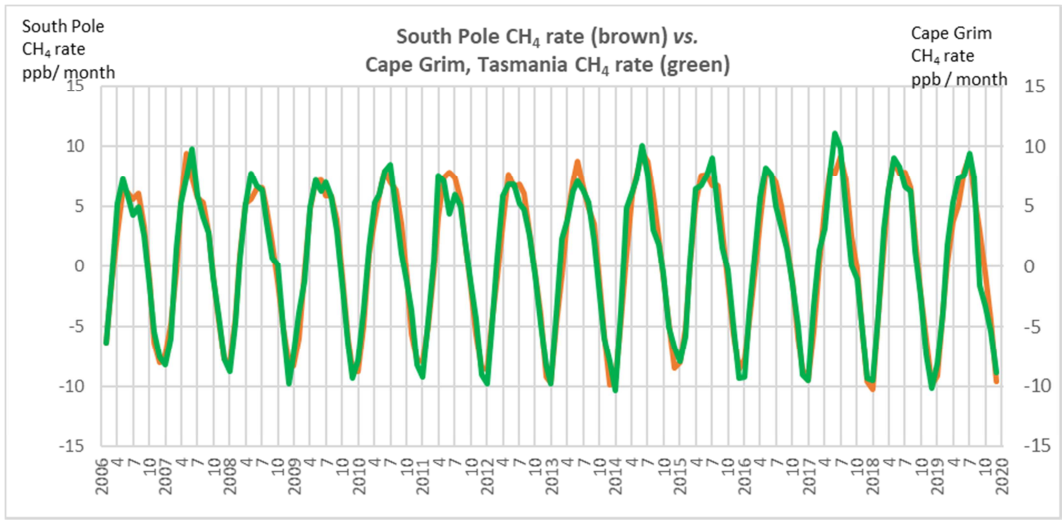

Figure 21. *Monthly methane rate South Pole vs. monthly methane rate Cape Grim (Tasmania).*

Time-series for Antarctic sea ice rate, a local temperature and South Pole methane rate are given in Figures 22-23.

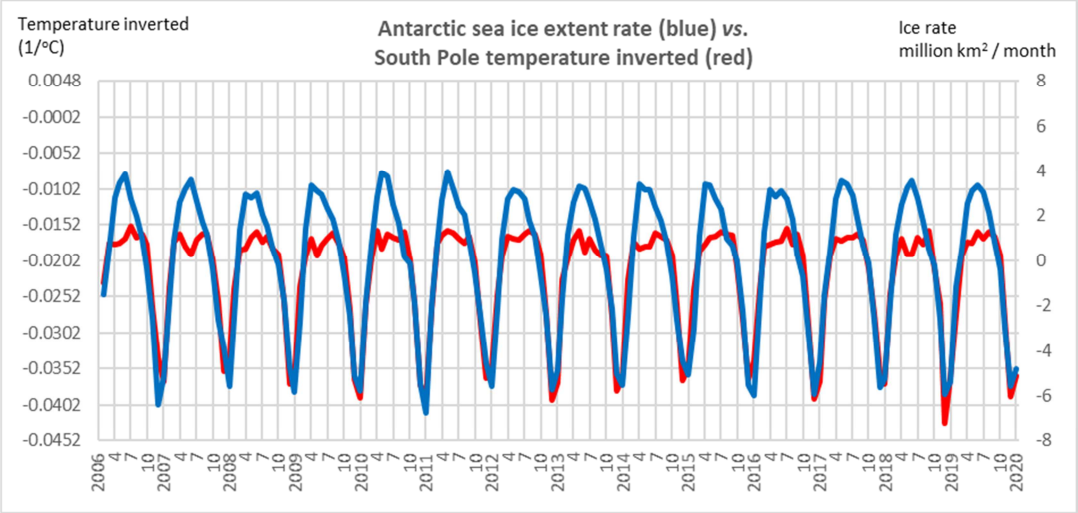

Figure 22. *Monthly Antarctic sea ice extent rate vs. temperature at South Pole (inverted).*

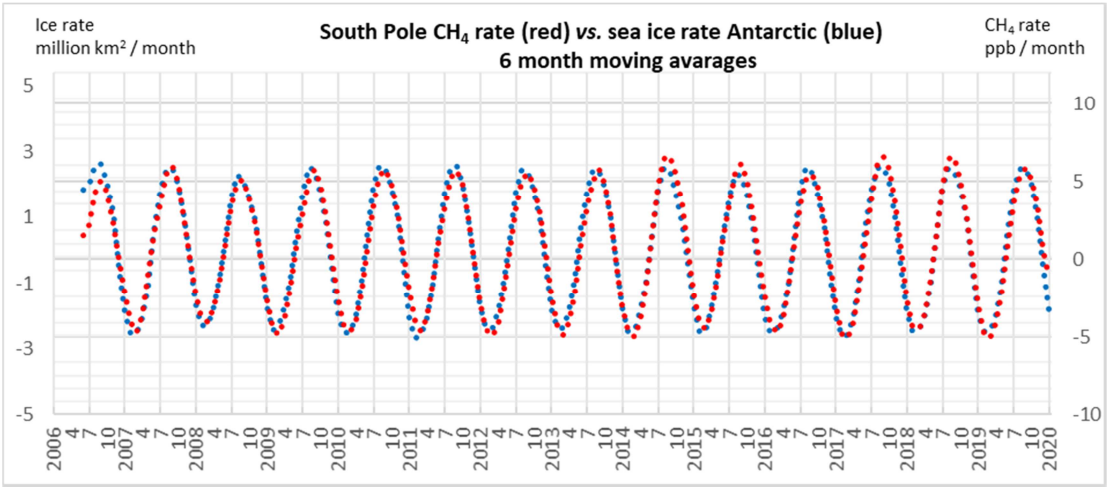

Figure 23. *Monthly Antarctic sea ice extent rate vs. monthly methane rate South Pole, 6 month moving average for both variables.*

d) Methyl chloroform and NDVI

Time-series for two variables usually assumed to drive methane and carbon dioxide dynamics are given in Figures 24-27.

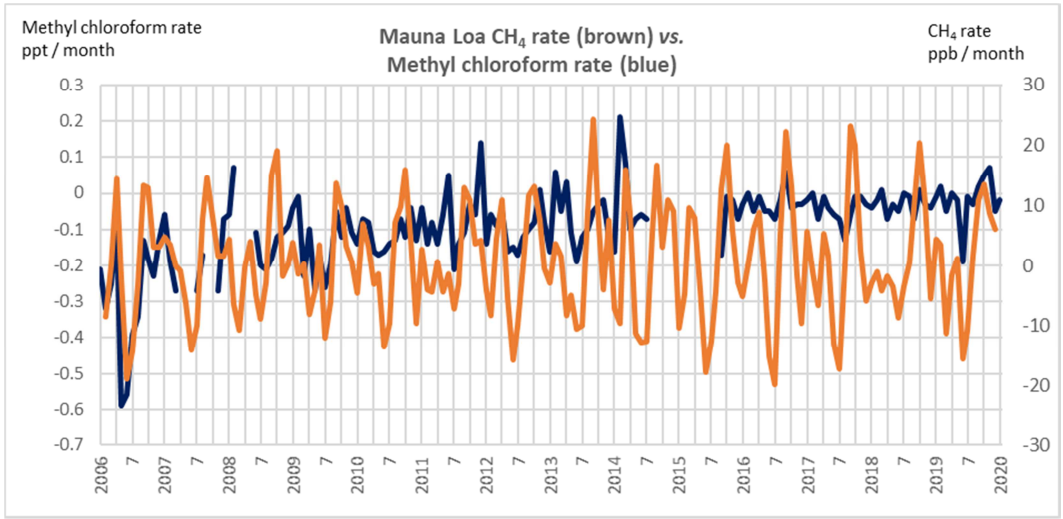

Figure 24. *Monthly methane rate Mauna Loa vs. monthly methyl chloroform rate Mauna Loa.*

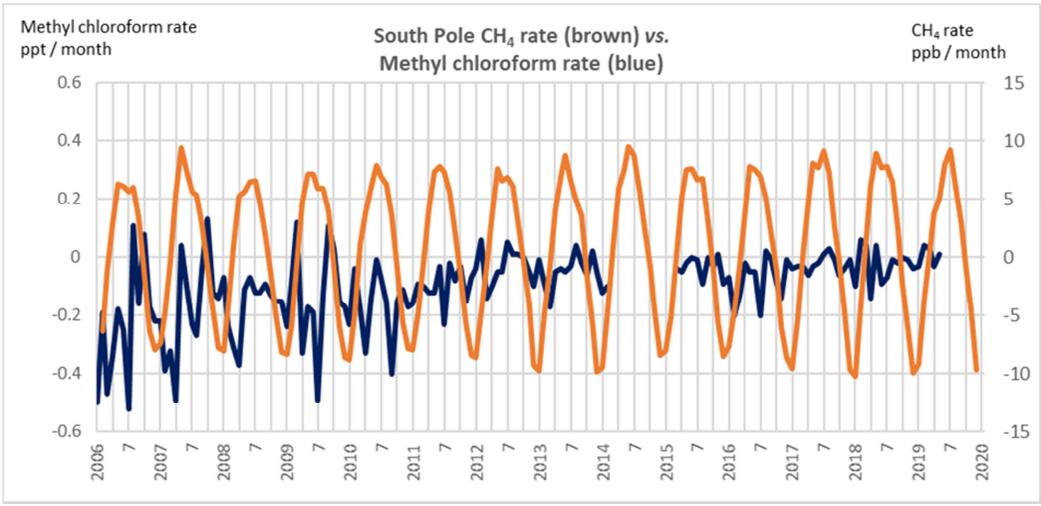

Figure 25. *Monthly methane rate South Pole vs. monthly methyl chloroform rate South Pole.*

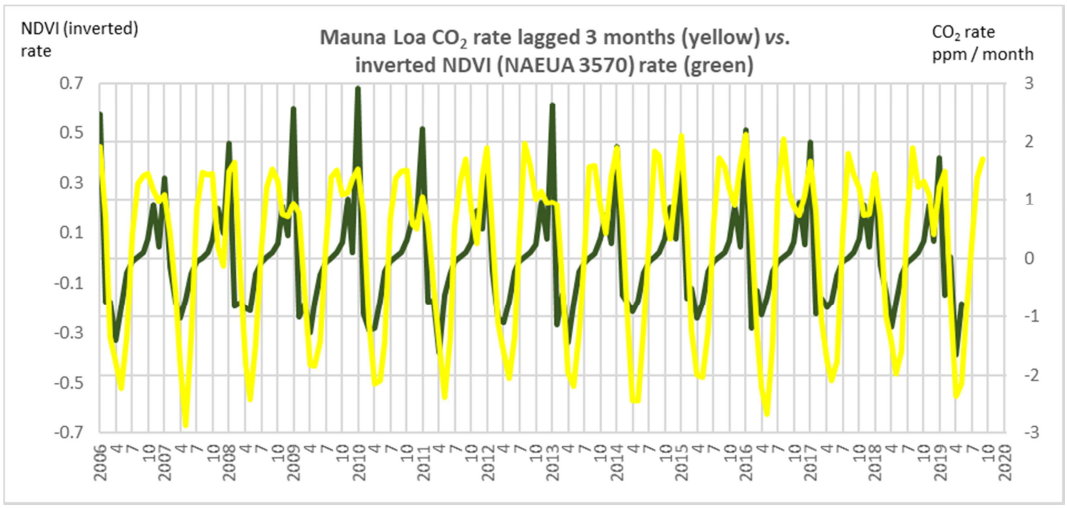

Figure 26. *Monthly carbon dioxide rate Mauna Loa (20°N) lagged 3 months vs. monthly inverted NDVI rate North America and Eurasia, 35°N to 70°N (NAEUA3570).*

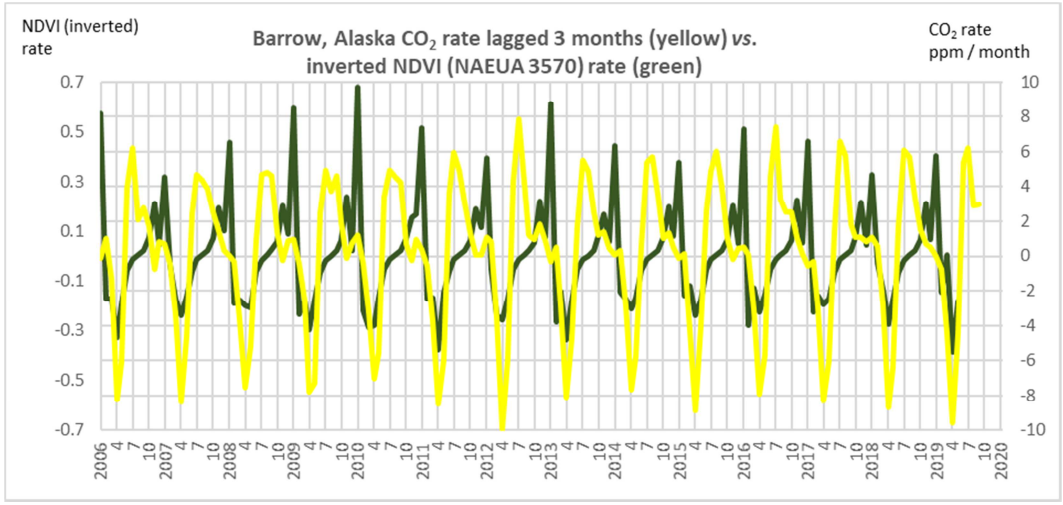

Figure 27. *Monthly carbon dioxide rate Barrow, Alaska (71°N) lagged 3 months vs. monthly inverted NDVI rate North America and Eurasia, 35°N to 70°N (NAEUA3570).*

e) Isotopes

Time-series for ^{13}C in CO_2 are plotted against those for potential drivers in Figures 28-31.

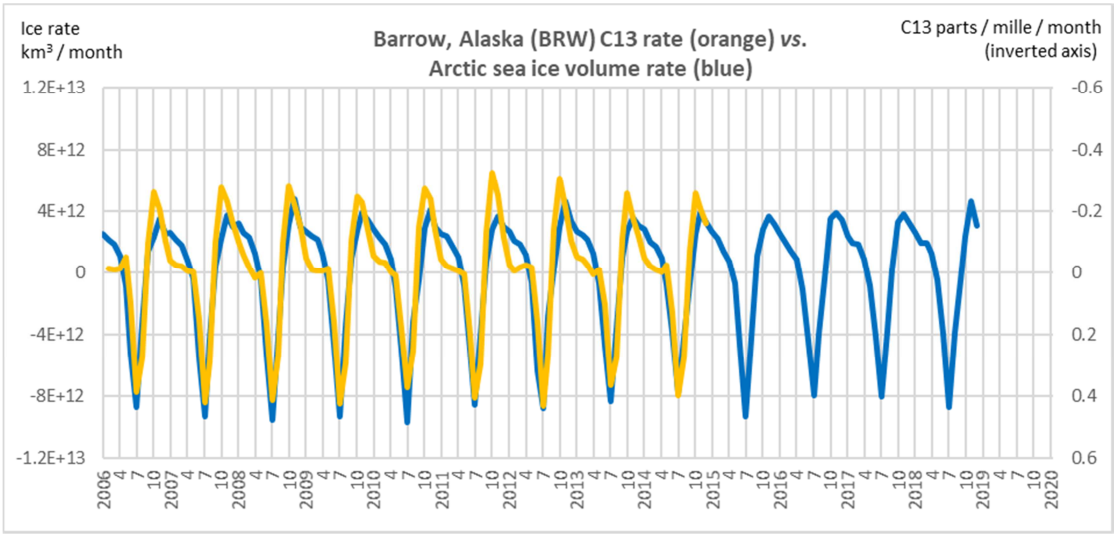

Figure 28. *Monthly $\delta^{13}C$ rate Barrow, Alaska (71°N) vs. Arctic sea ice volume rate.*

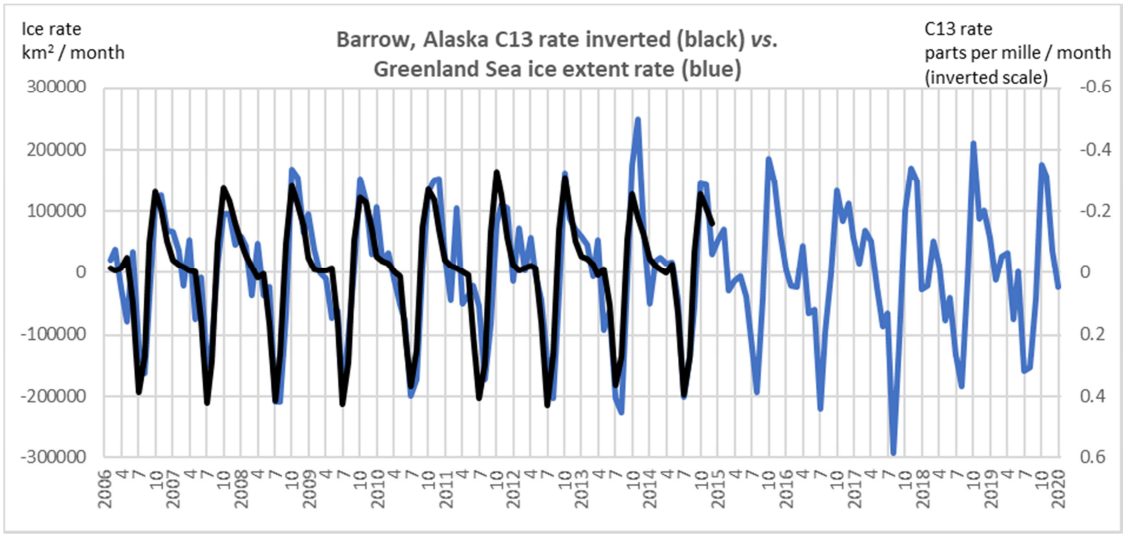

Figure 29. *Monthly $\delta^{13}C$ rate (in CO_2) Barrow, Alaska (inverted scale) vs. Greenland Sea ice extent rate.*

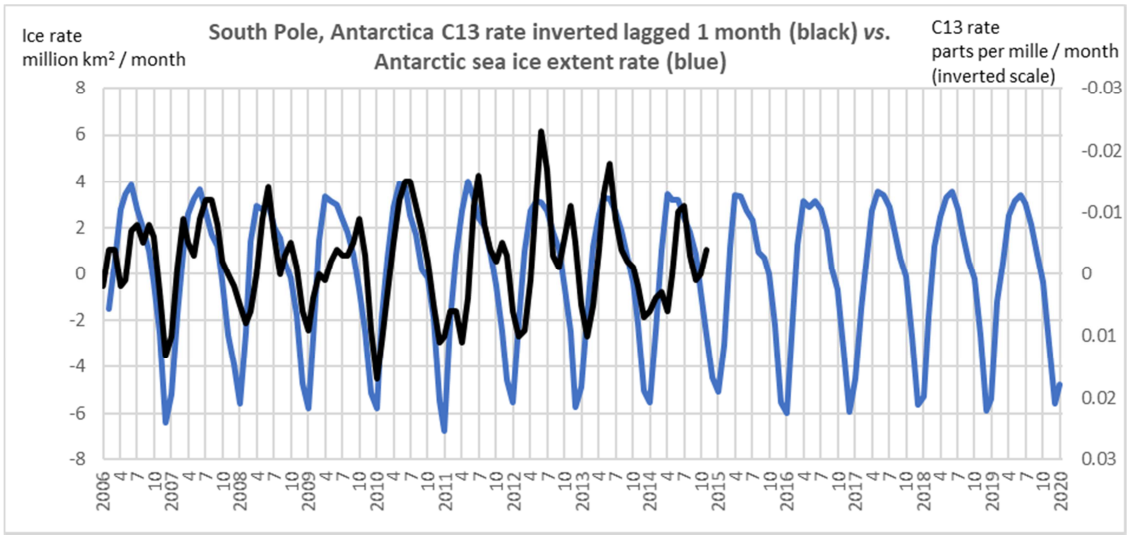

Figure 30. *Monthly $\delta^{13}C$ rate (in CO_2) South Pole (inverted scale, lagged one month) vs. Antarctic sea ice extent rate.*

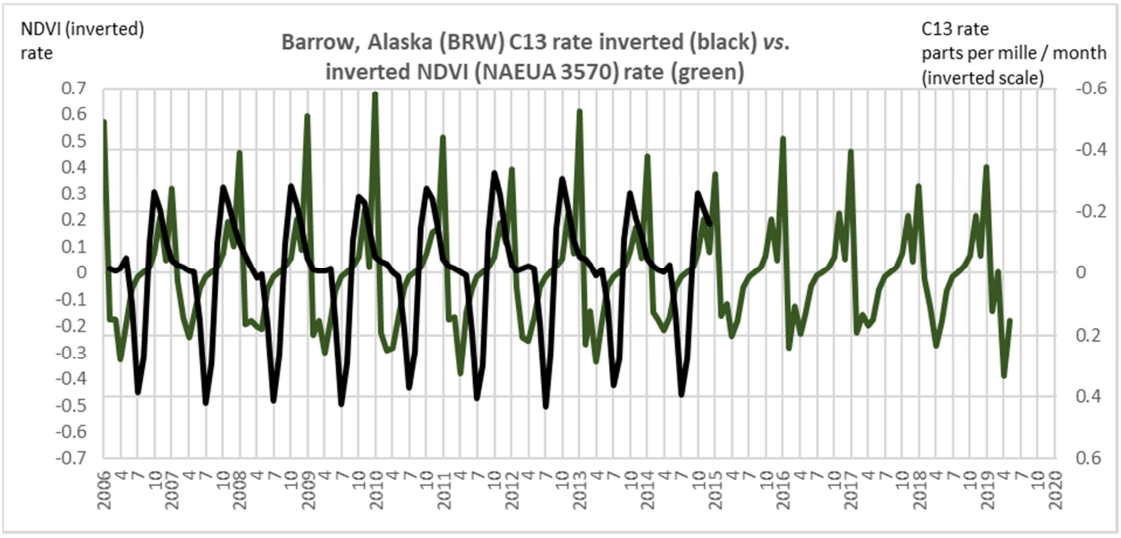

Figure 31. *Monthly $\delta^{13}C$ rate (in CO_2) Barrow, Alaska (71°N) (inverted scale) vs. monthly inverted NDVI rate North America and Eurasia, 35°N to 70°N (NAEUA3570).*

f) Annual changes in carbon dioxide

Annual changes in carbon dioxide rate are compared with annual changes in tropical ocean temperature anomaly in Figure 32. This measures acceleration or deceleration of the monthly carbon dioxide rate.

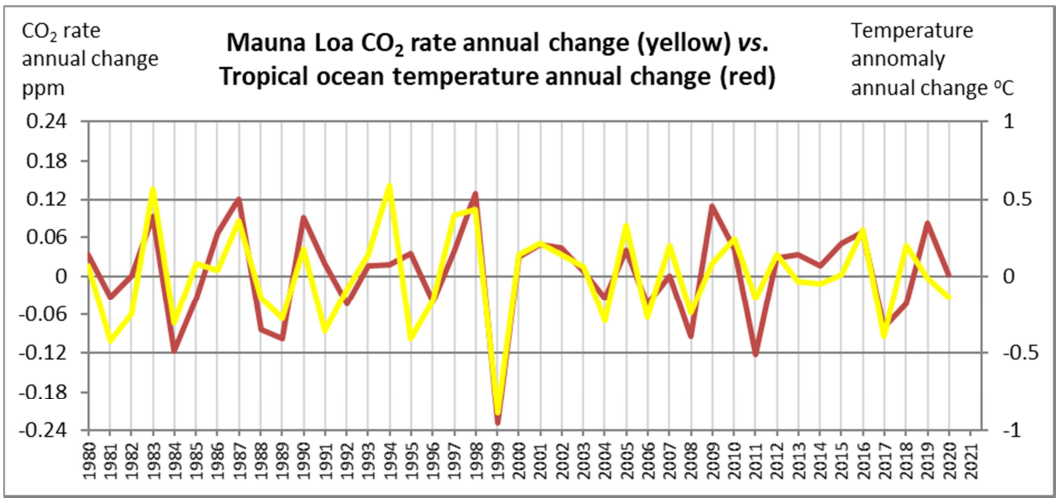

Figure 32. *Annual change in CO_2 rate vs. Annual change in Tropical ocean temperature anomaly. Derived from monthly averages. (Data accessed February 2022).*

4. Discussion

Since time-series of many phenomena with seasonal cycles will be correlated, often with lags, it is important to consider not only very high correlation coefficients but to carefully inspect the fine details of time-series for similarity of secondary peaks and troughs and for similarity of amplitudes within a yearly cycle.

Air temperature at or near the Poles peaks in very close synchrony with regional peaks in sea ice melt (Figures 16 and 22). It will also be correlated with a range of other abiotic and biotic variables with various lags, such as Northern Hemisphere snow (Figure 15) and Greenland terrestrial ice melt. Air temperature at high latitude sites leads the global carbon dioxide rate with a greater lag of carbon dioxide behind the Antarctic than the Arctic temperature (Figures 2-8).

The rates of change of globally representative levels of carbon dioxide and methane are very strongly correlated with the rate of change of global ('Arctic plus Antarctic') sea ice (Figures 1 and 9) on the timescales examined. The rate of change of methane at Mauna Loa has similar phenology but greater amplitude (Figure 10). The lag of 5 - 7 months between the peak Antarctic temperature (and sea ice melt) and the fastest decline of global methane and global carbon dioxide suggest a strong Antarctic influence on these gases (Figures 1 and 9). It may take months for the effects of temperature on gas flux in the Antarctic to reach the Northern Hemisphere or high altitudes.

The extremely strong predictive power of global total sea ice for carbon dioxide and methane is notable - revealing possible causality or high predictive power for the actual cause. The two peaks in global sea ice rate result from the peak temperatures in the two Hemispheres. Global carbon dioxide and methane rates also have twin peaks which are similarly separated (Figure 11). We propose that whatever dominates the fluxes of these gases makes strong contributions at high latitudes in both Hemispheres. For carbon dioxide we propose (on the basis of seasonal amplitudes and lags) that there is a particularly strong contribution from sea ice melt and calcium carbonate dissolution in the Greenland area [6].

Temperature in at least one Arctic recording site has a close synchrony with carbon dioxide (Figure 12) and methane (Figure 14) flux rates at the site (Alert, Canada). Carbon dioxide rate also shows remarkably high similarity to Greenland Sea ice extent rate, notably including the secondary peaks in the two time-series (Figure 13) which are more evident in Scripps data than NOAA carbon dioxide data [6]. Other high-latitude Northern Hemisphere recording sites in the NOAA network have similar carbon dioxide and methane phenology to Alert and Barrow [6, 7] suggesting large-scale synchrony.

Peak negative carbon dioxide flux (indicating drawdown or destruction of the gas) usually occurs synchronously with peak atmospheric temperature in the Arctic summer (July, Figure 12). This is also synchronous with peak decline in Arctic and Greenland sea ice extent (Figures 13 and 16). However, peak negative methane flux at Alert (Figure 14) occurs about one month earlier than peak temperature and peak sea ice melt in the whole Arctic, which we suggest results from an influence of the biota or other abiotic factors on methane dynamics in the Arctic. Arctic sea ice as a whole can not be the dominant causal variable in this region at least, but there are regional differences in sea ice phenology, and Alert methane peak decline is more closely synchronous with the Barents Sea ice rate (Hambler & Henderson, unpublished). Notably, the Barents Sea seabed and similar seabeds may be an underestimated substantive source of methane [26]. Peak rate of decline of Arctic methane is also closely synchronous with peak snow extent decline in the Northern Hemisphere, with Alert lagging snow melt rate by about a month (Figure 15), consistent with putative terrestrial influences such as increased methanogenic microbial activity. Peak methane emission from Arctic mires can occur near peak summer air temperature [49].

Peak negative methane flux at the South Pole is synchronous with peak temperature at the South Pole (Figures 19-20) but carbon dioxide rate at the South Pole lags one month behind the peak temperature which occurs December / January (Figure 18). Similarly, methane rates slightly lead carbon dioxide rates globally and at Mauna Loa (Figures 9-11). Intriguingly, South Pole temperature peaks simultaneously with peak rates of decline in both methane and carbon dioxide at the coastal and marine Antarctic sites in the NOAA network (Palmer, Syowa, Halley, Drake Passage) and is also simultaneous with peak Antarctic sea ice melt [6, 7]. There may be differential transport, production or removal processes for methane and carbon dioxide after a synchronous monthly pattern is imprinted in the two gases at the edge of the Antarctic continent. At the South Pole, methane rates are very highly synchronous with Antarctic sea ice extent rates (Figure 23). High latitude sites in the Southern Hemisphere have very similar methane phenology (*e.g.* Figure 21 and [7] suggesting a very well-mixed southern air mass (as per [3]) and / or a large-scale causal process.

The synchronous decline and rise in carbon dioxide and methane at many sites would most parsimoniously be explained by a single mechanism. These results are broadly consistent with our proposals that sea ice is either involved in the decline of atmospheric carbon dioxide and methane or is extremely strongly corelated with an unknown variable causing fluxes of the gases [6, 7]. We argue the extremely high correlations between sea ice and fluxes of both gases are more plausibly due to simple physical or chemical processes than to ecological ones [6, 7]. In particular, we suggest the peak negative gas rates may relate to ice melt and absorption by cold water undersaturated in these gases [50]. Similarly, ocean temperature was suggested to drive lagged carbon dioxide changes through solubility changes [34]. The peak positive rates may relate to expulsion of gas during sea ice formation (degassing), marine emissions during summer warming of the ocean and from upwelling, and other physical and biological processes [6, 7, 27, 51]. Mechanisms coupling sea ice and the atmosphere (such as brine drainage, modulation of upwelling, and ikaite dissolution cycles) are not yet well represented qualitatively or quantitatively in biogeochemical models [17, 27, 37, 51] and their magnitudes may have been underestimated.

High latitude oceans and sea ice are amongst the few places currently recorded as having frequent net emission of CO_2. Studies with emission and / or absorption phenologies we find broadly consistent with our hypothesis include: [27, 28, 52-73]. This selection of studies is not systematic but provides examples of fluxes and of the types of research that will be necessary to test predictions on representative spatial and temporal scales.

The conventional explanation of the terrestrial biota of the Northern Hemisphere driving the carbon dioxide seasonal cycle [1, 4, 9-14] does not explain the similar patterns of global carbon dioxide and methane which have many different biological and abiotic sources and sinks [1]. The similar patterns of seasonal variation of CO_2 concentration and ^{13}C isotopic fraction at several locations is puzzling if the fractionation mechanism is biotic and predominantly northern [11] but not if it is physical and the same in both Hemispheres. Some isotopes are in any case of limited use in identifying carbon fluxes because different sources can have the same fractions [36, 39].

Measured by NDVI, terrestrial productivity has relatively weak synchrony and curve shape similarity with carbon dioxide rates, in any large region, even with lags (Figures 26-

27; [6]), making this a less likely driver than sea ice rates despite common belief. For the period 2003-2018 inclusive, the cross correlation between sea ice volume and carbon dioxide rates ($r = 0.90$) is stronger than between NDVI (35°N -70°N) and carbon dioxide rates ($r = 0.62$) [6]. Alternatively, NDVI may be of limited value in detecting carbon fixation rates [74] despite its conventional use for this purpose - and dependence of flux on precipitation or other factors affecting productivity and respiration might be expected to introduce noise and weaken the relationship further. Terrestrial fluxes of carbon dioxide are not as well known as many imagine, and much recent data has been surprising [20] - as with periods of emission from tropical forests [75, 76] or large and seasonally complex fluxes over deserts [6, 77]. Those supporting the conventional 'consensus' view have yet to locate areas of the planet with such strong correlations as we find with global carbon dioxide rates - yet probably have an intuitive feeling such areas exist since this is easier to accept than to reject the current paradigm.

A major factor implicated in removing atmospheric methane, the hydroxyl radical (OH) [3, 39, 78, 79] is created by photodissociation and thus would be expected to be temperature-dependent with latitudinal variation in amplitude. Indeed, OH concentration is highest in the tropics [31, 47]. If as is widely assumed OH is dominant in global methane dynamics it would be expected to cause lagged fluxes of methane at the polar sites. The seasonal low of methane *level* near the South Pole occurs when OH is assumed high in the austral summer [3]. However, methane rate lags further behind peak temperature nearer the equator [7] suggesting net methane loss is not fastest where there is most sunlight. The relationship between methane rates and methyl chloroform rates is relatively weak (*e.g.* Figures 24-25 and Hambler & Henderson, unpublished). Moreover, to our knowledge there is no reported directly causal reason for OH to vary synchronously with carbon dioxide rate (as it often does regionally). Indeed, the positive modelled correlation between marine methane emission and photosynthetic productivity [21] would argue against synchrony with carbon dioxide release.

A lag of 7 months between temperature and carbon dioxide rate is consistent with the observed lag of about 9 - 10 months between temperature and carbon dioxide level [16, 80, 81], suggesting South Pole air temperature is a very good proxy for a variable driving the annual carbon cycle. South Pole air temperature and Antarctic sea ice extent rate should both have predictive power for the 'global' carbon dioxide level 10 months in advance. Our results are consistent with a proposed sequence of events driving carbon dioxide changes starting in the Southern Hemisphere [80], rather than the tropical land surface [16]. Tropical ocean temperature anomaly is also significantly coherent with lagged carbon dioxide level [34]. Temperature fluctuations at gridpoints in North East America and the North Atlantic but not polar regions were also significantly coherent with Mauna Loa carbon dioxide fluctuations [34]; it is possible the difference from our result reflects previous use of the Hadley Centre's HadCrut3 temperature anomaly rather than temperature, and carbon dioxide levels, rather than rates.

Isotope ratio rate for carbon dioxide clearly co-varies closely with sea ice rate (Figures 28-30) although these are not analysed statistically since the isotopic time-series is available for only part of the timeframe that we consider for carbon dioxide and methane. During sea ice formation in either hemisphere the ratio of ^{13}C to ^{12}C declines in the atmosphere; this is consistent with degassing of carbon dioxide enriched in ^{12}C, as demonstrated experimentally [38]. Notably, the transition dates between positive and negative rates are near synchronous for $\delta^{13}C$ and Arctic sea ice volume (Figure 28). The visual similarity between isotope rate and sea ice rate is closer for Barrow (Figure 29) than for the South Pole (Figure 30), and amplitudes are greater and more constant at Barrow. These features (and similar results for other polar sites, Hambler & Henderson unpublished) are consistent with fractionation being stronger in the Northern Hemisphere. At Barrow, there is an interesting close similarity of isotope rate to sea ice rate in the Greenland Sea (Figure 29), as there is with carbon dioxide rate and Greenland Sea ice rate (Figure 13; [6]).

In contrast to these near-simultaneous changes of rate of sea ice and isotopes, the northern photosynthetic rate of change, approximated by NDVI rate, does not have a closely similar pattern to $\delta^{13}C$ rate (Figure 31) with periods of fast $\delta^{13}C$ increase lagging fast increase photosynthetic activity by about 4 months. If photosynthetic rate and carbon dioxide rate were examined at numerous sites, non-synchrony might present a discriminating test of the seasonal source of enriched ^{13}C in carbon dioxide. The phenology of terrestrial respiration and decay releasing ^{12}C requires further investigation since peak fractionation rate may not coincide precisely with peak NDVI rate or peak NDVI.

Critiques of our methods and conclusions might suggest that there are stronger terrestrial flux correlations with the gas rates that have yet to be identified, and that the recorded quantities (moles) of carbon dioxide or methane in sea ice are insufficient to cause the global flux changes. Our results are indeed inconsistent with current estimates of gas budgets (*e.g.* [3, 5, 79]). Our response is that it is circular reasoning to use existing sampling of quantities and flux measurements to argue our predictions on under-sampled quantities must be wrong. Falsification of our hypotheses would require much more comprehensive spatial and temporal coverage of gas levels (such as satellites might provide). Whilst some carbon stores (such as in sea ice itself) might be lower than we predict, a combination of several temperature-dependent fluxes and stores in the carbon cycle might combine to reach the magnitudes required. Although sparse, many measurements of carbon dioxide phenology in polar regions show similar timings of positive and negative fluxes that are in general agreement with an involvement of sea ice and calcium carbonate (ikaite) dissolution [6, 51].

High temporal and spatial variability suggests determination of net annual flux from all regions will require hourly, or daily, consistent sampling at large scales and more

systematic analysis. Analyses and animations of the globe showing rates of change of gases, rather than levels, may be particularly informative and convincing; it is intriguing to see radiative forcing and/or carbon dioxide concentration peaking seasonally near the poles in a relatively spatially comprehensive analysis - which merits further serious investigation [82, 83].

Inter-annual variation in monthly rates leads to net accumulation or loss of methane and carbon dioxide from the atmosphere. Both the amplitude and phase of methane rates in many sites in the Southern Hemisphere south of about 25°S are very similar ([7] and *e.g.* Figure 21) suggesting large-scale common forcing. A variable such as temperature which correlates strongly with the amplitude of the annual cycle (*e.g.* Figures 19-20) could help explain net global trends: for example, warm years generally have higher sea ice melt rates and more negative gas rates which might be partially caused by dissolution in melt water and changes in upwelling of gas-laden water. Rapid change in the net flux of gas would be expected when the system is far from equilibrium, such as when ocean temperature is changing fast. We have found strong coherence between the change in the average rate of flux of carbon dioxide (*ie* acceleration or deceleration) and the rate of change of tropical ocean temperature (Figure 32). This is consistent with previous observations [6, 16, 34, 80].

The monthly time-series of sea ice extent we use (Table 1) are presumably created with relatively consistent methods between years but are only provided since 2006. There may be too little statistical power to examine in detail relationships between sea ice and annual rate - but we demonstrate [6] annual carbon dioxide rates correlate strongly with global and oceanic lower tropospheric temperature and thus mechanisms involving ice could be hypothesized. The selected longer time-series we have examined do not suggest recent years are anomalous (Figure 4; Figure 5; Figure 8; and Figure 20) and such longer series warrant further analysis. However, we have yet to find a strongly coherent relationship between sea ice and carbon dioxide flux (Hambler & Henderson, unpublished), suggesting the mechanism for net carbon dioxide accumulation in the atmosphere may not be dominated by that driving its annual cycle (as per [16]).

5. Conclusions

We suggest other variables be examined that might be influenced by temperature or insolation which might drive fluxes of carbon dioxide and methane. These include, for example, marine and terrestrial productivity, upwelling rates, sea temperature depth profiles, glacial and ice shelf melt and calving, winds, desert carbonate chemistry, and the hydroxyl radical (for methane). The factors driving the seasonal cycles may not dominate in the inter-year accumulation or loss of carbon dioxide and methane. Isolating the relative contributions of such factors would require far more data, although the sharp decline of atmospheric carbon dioxide and methane precisely at the time of peak ice melt suggests dissolution in temporarily cold water is a major component. However, our correlations between sea ice rates, carbon dioxide rates, methane rates are the strongest with a putative driver of global greenhouse gas dynamics that we are aware of - and we suggest they are a priority for further investigation and empirical tests of causality and mechanism. The global and Antarctic cycle of both gases have similarities suggesting the same processes or regions are involved in the dominant fluxes for both, despite their very different biological properties. Our results are consistent with stable isotopes of carbon in carbon dioxide being predominantly fractionated by sea ice formation and carbonate precipitation, rather than terrestrial photosynthesis as commonly believed; fractionation by freezing and other abiotic processes involving carbonates may have been underestimated (for example in [11]) and should be examined in the field and with satellites giving coverage of polar, lakes and desert regions.

If temperature drives the annual cycle of carbon dioxide and methane it should be no surprise if variation in temperature between years causes changes in the annual rate of accumulation or decline of these gases [6, 7]. Variation in the shape of the monthly temperature curve (*e.g.* Figure 8) can be used to predict variation in the monthly change of the gases - and hence monthly levels. A common mechanism could cause the observed similarity of long term changes in these gases [39, 81]. The phase relationship between temperature and carbon dioxide has been examined to help elucidate the possible direction of causality [16, 84-87] and the lags we find between time-series are consistent with carbon dioxide being the response variable. We suggest the temperature of the tropical ocean may be more important than that of the polar regions in net annual flux.

The current paradigm for the carbon cycle is supported by weaker correlations than the paradigm we propose. In summary, our proposed paradigm is that the high latitude oceans are a net source of atmospheric carbon dioxide and methane due to outgassing and upwelling, punctuated annually by a brief period of oceanic drawdown when ice melts and cold water absorbs gases and impedes upwelling. Whilst paradigm shifts require strong evidence, a failure to thoroughly explore the strongest correlations would be scientifically negligent. If potential processes with appropriately large magnitudes are discovered though correlations, large scale experiments will be needed to test causation. Given the high economic, social and environmental costs [88] of attempting to manipulate the flux of greenhouse gases it is paramount that natural fluxes be identified and partitioned to deduce the relative scale of human influence upon them.

Data Availability Statement

Data are available from the sources in Table 1.

Author Contributions

CH and PAH contributed equally to the theory and discussion. CH performed most of the literature review, data compilation and graphics. PAH performed the statistical analysis.

Declarations

Conflict of Interest / Competing Interest Statement

The authors have no conflict of interest / competing interests.

Data Availability Statement

Data are available from the online providers indicated in Table 1. R code can be provided upon reasonable request.

Acknowledgements

Download and processing of MODIS satellite imagery was implemented by Environmental Research Group Oxford, Ltd. and we thank William Wint for this and for critical comment. Several colleagues and particularly Marian Dawkins provided valuable critiques. We thank all sources listed in Table 1 or indicated in the metadata on the hosting websites: the effort of collecting and curating valuable long-term data is enormous.

References

[1] IPCC (2013) Climate Change 2013: The physical science basis. Contribution of Working Group I to the Fifth Assessment Report of the Intergovernmental Panel on Climate Change (ed. by T. Stocker, D. Qin, G.-K. Plattner et al), Cambridge University Press, Cambridge, United Kingdom.

[2] Fung, I., John, J., Lerner, J. et al (1991) Three-dimensional model synthesis of the global methane cycle. Journal of Geophysical Research, 96, 13033-13065. https://doi.org/10.1029/91JD01247

[3] Dlugokencky, E. J., Steele, L., Lang, P. M. et al (1994) The growth rate and distribution of atmospheric methane. Journal of Geophysical Research: Atmospheres, 99, 17021-17043. https://doi.org/10.1029/94JD01245

[4] He, Z., Zeng, Z. C., Lei, L. P. et al (2017) A data-driven assessment of biosphere-atmosphere interaction impact on seasonal cycle patterns of XCO_2 Using GOSAT and MODIS observations. Remote Sensing, 9, 251. https://doi.org/10.3390/rs9030251

[5] Saunois, M., Stavert, A., Poulter, B. et al (2020) The Global Methane Budget 2000-2017. Earth System Science Data, 12, 1561-1623. https://doi.org/10.5194/ESSD-12-1561-2020

[6] Hambler, C. & Henderson, P. A. (2020) Sea ice and carbon dioxide. Working Paper, version 2. https://ora.ox.ac.uk/objects/uuid:640a0c7e-6b55-4aff-a9cc-f47f6b490254

[7] Hambler, C. & Henderson, P. A. (2020) Sea ice and methane. Working paper, version 2. https://ora.ox.ac.uk/objects/uuid:52b0e80f-7358-4b88-8941-55068738638e

[8] Heimann, M., Keeling, C. D. & Tucker, C. J. (1989) A three-dimensional model of atmospheric CO_2 transport based on observed winds: 3. Seasonal cycle and synoptic time scale variations. Aspects of climate variability in the Pacific and the Western Americas, Geophysical Monograph, 55, 277-303. https://doi.org/10.1029/GM055p0277

[9] Keeling, C. D., Bacastow, R. B., Carter, A. et al (1989) A three-dimensional model of atmospheric CO_2 transport based on observed winds: 4. Mean annual gradients and interannual variations. Aspects of climate variability in the Pacific and the Western Americas, Geophysical Monograph, 55, 305-363. https://doi.org/10.1029/GM055p0305

[10] Keeling, C. D., Piper, S. C., Bacastow, R. B. et al (2001) Exchanges of atmospheric CO_2 and $^{13}CO_2$ with the terrestrial biosphere and oceans from 1978 to 2000. In: Exchanges of atmospheric CO_2 and $^{13}CO_2$ with the terrestrial biosphere and oceans from 1978 to 2000. I. Global aspects, SIO Reference Series, No. 01-06, pp. 1-88. Scripps Institution of Oceanography, San Diego.

[11] Keeling, C. D., Piper, S. C., Bacastow, R. B. et al (2005) Atmospheric CO_2 and $^{13}CO_2$ exchange with the terrestrial biosphere and oceans from 1978 to 2000: observations and carbon cycle implications. In: A history of atmospheric CO_2 and its effects on plants, animals, and ecosystems. Ecological Studies (Analysis and Synthesis) (ed. by I. Baldwin et al), 177, pp. 83-133. Springer, New York. https://doi.org/10.1007/0-387-27048-5_5

[12] Buermann, W., Lintner, B. R., Koven, C. D. et al (2007) The changing carbon cycle at Mauna Loa Observatory. Proceedings of the National Academy of Sciences, 104, 4249-4254. https://doi.org/10.1073/pnas.0611224104

[13] Keeling, R. F. (2008) Recording Earth's vital signs. Science, 319, 1771-1772. https://doi.org/10.1126/science.1156761

[14] Jiang, X. & Yung, Y. L. (2019) Global patterns of carbon dioxide variability from satellite observations. Annual Review of Earth and Planetary Sciences, 47, 225-245. https://doi.org/10.1146/annurev-earth-053018-060447

[15] Nelson, M. D. & Nelson, D. B. (2016) Oceans, ice & snow and CO_2 rise, swing and seasonal fluctuation. International Journal of Geosciences, 7, 1232-1282. https://doi.org/10.4236/ijg.2016.710092

[16] Salby, M. & Harde, H. (2022) Control of atmospheric CO_2. Part II: Influence of tropical warming. Science of Climate Change, 1, N2 1-29. https://doi.org/10.53234/scc202112/211

[17] Kort, E. A., Wofsy, S. C., Daube, B. C. et al (2012) Atmospheric observations of Arctic Ocean methane emissions up to 82 degrees north. Nature Geoscience, 5, 318-321. https://doi.org/10.1038/ngeo1452

[18] Zhao, F., Zeng, N., Asrar, G. et al (2016) Role of CO_2, climate and land use in regulating the seasonal amplitude increase of carbon fluxes in terrestrial ecosystems: a multimodel analysis. Biogeosciences, 13, 5121–5137. https://doi.org/10.5194/bg-13-5121-2016

[19] Resplandy, L., Keeling, R. F., Rödenbeck, C. et al (2018) Revision of global carbon fluxes based on a reassessment of oceanic and riverine carbon transport. Nature Geoscience, 11, 504-509. https://doi.org/10.1038/s41561-018-0151-3

[20] Palmer, P. I., Feng, L, Baker, D. et al (2019) Net carbon emissions from African biosphere dominate pan-tropical atmospheric CO_2 signal. Nature Communications 10, Article number: 3344 (2019). https://doi.org/10.1038/s41467-019-11097-w

[21] Weber, T., Wiseman, N. A. & Kock, A. (2019) Global ocean methane emissions dominated by shallow coastal waters. Nature Communications, 10, 4584. https://doi.org/10.1038/s41467-019-12541-7

[22] Winkler, A. J., Myneni, R. B., Alexandrov, G. A. et al (2019) Earth system models underestimate carbon fixation by plants in the high latitudes. Nature Communications, 10, 1-8. https://doi.org/10.1038/s41467-019-08633-z

[23] Green, J. K., Berry, J, Ciais, P. et al (2020) Amazon rainforest photosynthesis increases in response to atmospheric dryness. Science Advances 6, No 47. https://www.science.org/doi/10.1126/sciadv.abb7232

[24] Copernicus (2019) https://atmosphere.copernicus.eu/new-high-quality-cams-maps-carbon-dioxide-surface-fluxes-obtained-satellite-observations.

[25] Harris, N. L., Gibbs, D. A., Baccini, A. et al (2021) Global maps of twenty-first century forest carbon fluxes. Nature Climate Change, 11, 234–240. https://doi.org/10.1038/s41558-020-00976-6

[26] Serov, P, Mattingsdal, R., Winsborrow, M. et al (2022) Widespread natural methane and oil leakage from sub-marine Arctic reservoirs. Research Square. https://doi.org/10.21203/rs.3.rs-1225012/v1

[27] Vancoppenolle, M. & Tedesco, L. (2016) Numerical models of sea ice biogeochemistry. In: Sea ice, 3rd edn. (ed. by D. N. Thomas), pp. 492-515. Wiley, New Jersey. https://doi.org/10.1002/9781118778371.ch20

[28] Geilfus, N.-X., Pind, M. L., Else, B. G. T. et al (2018) Spatial and temporal variability of seawater pCO_2 within the Canadian Arctic Archipelago and Baffin Bay during the summer and autumn 2011. Continental Shelf Research, 156, 1-10. https://doi.org/10.1016/j.csr.2018.01.006

[29] Bushinsky, S. M., Landschützer, P., Rödenbeck, C. et al (2019) Reassessing Southern Ocean air sea CO_2 flux estimates with the addition of biogeochemical float observations. Global Biogeochemical Cycles, 33, 1370-1388. https://doi.org/10.1029/2019GB006176

[30] MOSAiC (2019) The key to the Arctic puzzle. From https://www.mosaic-expedition.org/science/arctic-climate/. Accessed 29 October 2019.

[31] Hein, R., Crutzen, P. J. & Heimann, M. (1997) An inverse modelling approach to investigate the global atmospheric methane cycle. Global Biogeochemical Cycles, 11, 43-76. https://doi.org/10.1029/96GB03043

[32] Beer, C., Reichstein, M., Tomelleri, E. et al (2010) Terrestrial gross carbon dioxide uptake: global distribution and covariation with climate. Science, 329, 834-838. https://doi.org/10.1126/science.1184984

[33] Sitch, S., Friedlingstein, P., Gruber, N. et al (2015) Recent trends and drivers of regional sources and sinks of carbon dioxide. Biogeosciences, 12, 653-679. https://doi.org/10.5194/bg-12-653-2015

[34] Park, J. (2009) A re-evaluation of the coherence between global-average atmospheric CO_2 and temperatures at interannual time scales. Geophysical Research Letters, 36, L22704. https://doi.org/10.1029/2009GL040975

[35] IPCC (in press) Climate Change 2021: The Physical Science Basis. Contribution of Working Group I to the Sixth Assessment Report of the Intergovernmental Panel on Climate Change (ed by V. Masson-Delmotte, P. Zhai, A. Pirani et al), Cambridge University Press, Cambridge, United Kingdom.

[36] Salby, M. & Harde, H. (2021) Control of atmospheric CO_2. Part I: Relation of Carbon 14 to the removal of CO_2. Science of Climate Change, 1, N1 1-36. https://doi.org/10.53234/scc202112/210

[37] Damm, E., Rudels, B., Schauer, U. et al (2015) Methane excess in Arctic surface water - triggered by sea ice formation and melting. Scientific Reports, 5, 16179. https://doi.org/10.1038/srep16179

[38] Niles, P. B., Socki, R. A. & Hredzak, P. L. (2007) A new method for evaluating the carbon isotope characteristics of carbonate formed under cryogenic conditions analogous to Mars. Lunar and Planetary Science, XXXVIII.

[39] Salby, M. (2012) Physics of the atmosphere and climate, 2nd edn. Cambridge University Press, Cambridge, United Kingdom. https://doi.org/10.1017/CBO9781139005265

[40] Dlugokencky, E. J., Mund, J. W., Crotwell, A. M. et al (2020) Atmospheric carbon dioxide dry air mole fractions from the NOAA GML Carbon Cycle Cooperative Global Air Sampling Network, 1968-2019, Version: 2020-07. https://doi. org/10. 15138/wkgj-f215. Accessed 1 August 2020.

[41] Dlugokencky, E. J., Crotwell, A. M., Mund, J. W. et al (2020) Atmospheric methane dry air mole fractions from the NOAA GML Carbon Cycle Cooperative Global Air Sampling Network, 1983-2019, Version: 2020-07, https://doi.org/10.15138/VNCZ-M766. Accessed 1 August 2020.

[42] Dlugokencky, E. (2021) Ed Dlugokencky, NOAA/GML (www.esrl.noaa.gov/gmd/ccgg/trends_ch4/). Accessed 1 January 2021.

[43] White, J. W. C., Vaughn B. H. & Michel, S. E. (2015) University of Colorado, Institute of Arctic and Alpine Research (INSTAAR), Stable Isotopic Composition of Atmospheric Carbon Dioxide (13C and 18O) from the NOAA ESRL Carbon Cycle Cooperative Global Air Sampling Network, 1990-2014, Version: 2015-10-26, Path: ftp://aftp.cmdl.noaa.gov/data/trace_gases/co2c13/flask/

[44] Fetterer, F., Knowles, K., Meier, W. N. et al (2017) Updated daily. Sea Ice Index, Version 3. monthly North and South. Boulder, Colorado USA. NSIDC: National Snow and Ice Data Center. https://doi.org/10.7265/N5K072F8. Accessed 26 February 2020.

[45] Spencer, R., Christy, J. & Braswell, W. (2015) Version 6. 0 of the UAH Temperature Dataset Released: New LT Trend = +0. 11 C/decade. https://www.drroyspencer.com/2015/04/version-6-0-of-the-uah-temperature-dataset-released-new-lt-trend-0-11-cdecade/.

[46] Ravishankara, A. R. & Albritton, D. L. (1995) Methyl chloroform and the atmosphere. Science, 269, 183-184. https://doi.org/10.1126/science.269.5221.183

[47] Reidel, K. & Lassey, K. (2008) "Detergent of the atmosphere". Water & Atmosphere, 16, 22-23.

[48] Henderson, P. A. (2021) Southwood's Ecological Methods. 5th Edn. Oxford University Press, Oxford, United Kingdom. https://doi.org/10.1093/oso/9780198862277.001.0001

[49] Jackowicz-Korczyński, M., Christensen, T. R., Bäckstrand, K. et al (2010) Annual cycle of methane emission from a subarctic peatland. Journal of Geophysical Research: Biogeosciences, 115, G02009. https://doi.org/10.1029/2008JG000913

[50] Wiesenburg, D. A. & Guinasso Jr, N. L. (1979) Equilibrium solubilities of methane, carbon monoxide, and hydrogen in water and sea water. Journal of Chemical and Engineering Data, 24, 356-360. https://doi.org/10.1021/je60083a006

[51] Vancoppenolle, M., Meiners, K. M., Michel, C. et al (2013) Role of sea ice in global biogeochemical cycles: emerging views and challenges. Quaternary Science Reviews, 79, 207-230. https://doi.org/10.1016/j.quascirev.2013.04.011

[52] Ishii, M., Inoue, H. Y. & Matsueda, H. (2002) Net community production in the marginal ice zone and its importance for the variability of the oceanic pCO2 in the Southern Ocean south of Australia. Deep Sea Research Part II: Topical Studies in Oceanography, 49, 1691-1706. https://doi.org/10.1016/S0967-0645(02)00007-3

[53] Semiletov, I. P., Pipko, I. I., Repina, I. et al (2007) Carbonate chemistry dynamics and carbon dioxide fluxes across the atmosphere–ice–water interfaces in the Arctic Ocean: Pacific sector of the Arctic. Journal of Marine Systems, 66, 204-226. https://doi.org/10.1016/j.jmarsys.2006.05.012

[54] Bakker, D., Hoppema, M., Schröder, M. et al (2008) A rapid transition from ice covered CO_2-rich waters to a biologically mediated CO_2 sink in the eastern Weddell Gyre. Biosciences, 5, 1373-1386. https://doi.org/10.5194/bg-5-1373-2008

[55] Nomura, D., Eicken, H., Gradinger, R. et al (2010) Rapid physically driven inversion of the air–sea ice CO_2 flux in the seasonal landfast ice off Barrow, Alaska after onset of surface melt. Continental Shelf Research, 30, 1998-2004. https://doi.org/10.1016/j.csr.2010.09.014

[56] Nomura, D., Granskog, M. A., Assmy, P. et al (2013) Arctic and Antarctic sea ice acts as a sink for atmospheric CO_2 during periods of snowmelt and surface flooding. Journal of Geophysical Research: Oceans, 118, 6511-6524. https://doi.org/10.1002/2013JC009048

[57] Nomura, D., Yoshikawa-Inoue, H., Kobayashi, S. et al (2014) Winter-to-summer evolution of pCO_2 in surface water and air–sea CO_2 flux in the seasonal ice zone of the Southern Ocean. Biogeosciences, 11, 5749-5761. https://doi.org/10.5194/bg-11-5749-2014

[58] Nomura, D., Granskog, M. A., Fransson, A. et al (2018) CO_2 flux over young and snow-covered Arctic pack ice in winter and spring. Biogeosciences, 15, 3331-3343. https://doi.org/10.5194/bg-15-3331-2018

[59] Sejr, M. K., Krause-Jensen, D., Rysgaard, S. et al (2011) Air-sea flux of CO_2 in Arctic coastal waters influenced by glacial melt water and sea ice. Tellus B: Chemical and Physical Meteorology, 63, 815-822. https://doi.org/10.1111/j.1600-0889.2011.00540.x

[60] Fransson, A., Chierici, M., Yager, P. L. et al (2011) Antarctic sea ice carbon dioxide system and controls. Journal of Geophysical Research: Oceans, 116, C12035. https://doi.org/10.1029/2010JC006844

[61] Fransson, A., Chierici, M., Skjelvan, I. et al (2017) Effects of sea-ice and biogeochemical processes and storms on under-ice water fCO_2 during the winter-spring transition in the high Arctic Ocean: Implications for sea-air CO_2 fluxes. Journal of Geophysical Research: Oceans, 122, 5566-5587. https://doi.org/10.1002/2016JC012478

[62] Shadwick, E. H., Thomas, H., Chierici, M. et al (2011) Seasonal variability of the inorganic carbon system in the Amundsen Gulf region of the southeastern Beaufort Sea. Limnology and Oceanography, 56, 303-322. https://doi.org/10.4319/lo.2011.56.1.0303

[63] Geilfus, N.-X., Carnat, G., Dieckmann, G. S. et al (2013) First estimates of the contribution of $CaCO_3$ precipitation to the release of CO_2 to the atmosphere during young sea ice growth. Journal of Geophysical Research: Oceans, 118, 244-255. https://doi.org/10.1029/2012JC007980

[64] Geilfus, N.-X., Tison, J. -L., Ackley, S. et al (2014) Sea ice pCO_2 dynamics and air–ice CO_2 fluxes during the Sea Ice Mass Balance in the Antarctic (SIMBA) experiment–Bellingshausen Sea, Antarctica. Cryosphere, 8, 2395-2407. https://doi.org/10.5194/tc-8-2395-2014

[65] Geilfus, N.-X., Galley, R. J., Crabeck, O. et al (2015) Inorganic carbon dynamics of melt-pond-covered first-year sea ice in the Canadian Arctic. Biogeosciences, 12, 2047-2061. https://doi.org/10.5194/bg-12-2047-2015

[66] Roden, N. P., Tilbrook, B., Trull, T. W. et al (2016) Carbon cycling dynamics in the seasonal sea ice zone of East Antarctica. Journal of Geophysical Research: Oceans, 121, 8749-8769. https://doi.org/10.1002/2016JC012008

[67] Brown, K. A., Miller, L. A., Mundy, C. J. et al (2015) Inorganic carbon system dynamics in landfast Arctic sea ice during the early-melt period. Journal of Geophysical Research: Oceans, 120, 3542-3566. https://doi.org/10.1002/2014JC010620

[68] Butterworth, B. J. & Miller, S. D. (2016) Air-sea exchange of carbon dioxide in the Southern Ocean and Antarctic marginal ice zone. Geophysical Research Letters, 43, 7223-7230. https://doi.org/10.1002/2016GL069581

[69] Prytherch, J., Brooks, I. M., Crill, P. M. et al (2017) Direct determination of the air-sea CO_2 gas transfer velocity in Arctic sea ice regions. Geophysical Research Letters, 44, 3770-3778. https://doi.org/10.1002/2017GL073593

[70] Tison, J.-L., Delille, B. & Papadimitriou, S. (2016) Gases in sea ice. In: Sea ice, 3rd edn. (ed. by D. N. Thomas), pp. 433-471. Wiley, New Jersey. https://doi.org/10.1002/9781118778371.ch18

[71] Gray, A. R., Johnson, K. S., Bushinsky, S. M. et al (2018) Autonomous biogeochemical floats detect significant carbon dioxide outgassing in the high latitude Southern Ocean. Geophysical Research Letters, 45, 9049-9057. https://doi.org/10.1029/2018GL078013

[72] Søgaard, D. H., Deming, J. W., Meire, L. et al (2019) Effects of microbial processes and $CaCO_3$ dynamics on inorganic carbon cycling in snow-covered Arctic winter sea ice. Marine Ecology Progress Series, 611, 31-44. https://doi.org/10.3354/meps12868

[73] Ouyang, Z., Qi, D., Chen, L. et al. (2020) Sea-ice loss amplifies summertime decadal CO_2 increase in the western Arctic Ocean, Nature Climate Change. https://doi.org/10.1038/s41558-020-0784-2

[74] Welp, L. R., Patra, P. K., Rödenbeck, C. et al (2016) Increasing summer net CO_2 uptake in high northern ecosystems inferred from atmospheric inversions and comparisons to remote-sensing NDVI. Atmospheric Chemistry and Physics, 16, 9047-9066. https://doi.org/10.5194/acp-16-9047-2016

[75] Qin, Y., Xiao, X., Wigneron, J.-P. et al (2021) Carbon loss from forest degradation exceeds that from deforestation in the Brazilian Amazon. Nature Climate Change 11, 442-48. https://doi.org/10.1038/s41558-021-01026-5

[76] UNESCO, WRI, IUCN (2021) World Heritage forests: Carbon sinks under pressure. UNESCO, Paris.

[77] Mearns, E. (2015) CO2 - The view from space - update. http://euanmearns.com/co2-the-view-from-space-update/ Accessed 24 April 2021.

[78] Mastepanov, M., Sigsgaard, C., Dlugokencky, E. J. et al (2008) Large tundra methane burst during onset of freezing. Nature, 456, 628–630. https://doi.org/10.1038/nature07464

[79] Ciais, P., Sabine, C., Bala, G. et al (2013) Carbon and other biogeochemical cycles. In: Climate change 2013: the physical science basis. Contribution of Working Group I to the Fifth Assessment Report of the Intergovernmental Panel on Climate Change (ed. by T. Stocker, D. Qin, G.-K. Plattner et al), pp. 465-570. Cambridge University Press, Cambridge, United Kingdom.

[80] Humlum, O., Stordahl, K. & Solheim, J.-E. (2013) The phase relation between atmospheric carbon dioxide and global temperature. Global and Planetary Change, 100, 51-69. https://doi.org/10.1016/j.gloplacha.2012.08.008

[81] Salby, M. (2013) Presentation Prof. Murry Salby in Hamburg on 18 April 2013. https://web.archive.org/web/20150827075724/https://www.youtube.com/watch?v=2ROw_cDKwc0&feature=youtu.be. Accessed 14 June 2022.

[82] Rentsch, C. (2021) https://twitter.com/crentsch/status/1358122750259441666

[83] Rentsch, C. (2021) Radiative forcing by CO_2 observed at top of atmosphere from 2002-2019. https://doi.org/10.48550/arXiv.1911.10605

[84] Granger, C. W. J. (1969) Investigating causal relations by econometric models and cross-spectral methods. Econometrica, 37, 424-438. https://doi.org/10.2307/1912791

[85] Stips, A., Macias, D., Coughlan, C. et al (2016) On the causal structure between CO_2 and global temperature. Scientific Reports, 6, 1-9. https://doi.org/10.1038/srep21691

[86] Faes, L., Nollo, G., Stramaglia, S. et al (2017) Multiscale Granger causality. Physical Review E, 96, 042150. https://doi.org/10.1103/PhysRevE.96.042150

[87] Koutsoyiannis, D, Onof, C., Christofidis, A. et al (2022) Revisiting causality using stochastics: 2. Applications. Proceedings of the Royal Society A, 478, 20210836. https://doi.org/10.1098/rspa.2021.0836

[88] Hambler, C. & Canney, S. M. (2013) Conservation. 2nd Edn. Cambridge University Press, Cambridge, United Kingdom. https://doi.org/10.1017/CBO9780511792472